Supporting Information RASPA3: A Monte Carlo Code for Computing Adsorption and Diffusion in Nanoporous Materials and Thermodynamics Properties of Fluids

Y.A. Ran,[1] S. Sharma,[2] S.R.G. Balestra,[3] Z. Li,[4] S. Calero,[5] T.J.H Vlugt,[2] R.Q. Snurr,[4] and D. Dubbeldam[1, a)]

[1)]*Van 't Hoff Institute for Molecular Sciences, University of Amsterdam Science Park 904, 1098 XH Amsterdam (The Netherlands).*

[2)]*Engineering Thermodynamics, Process & Energy Department, Faculty of Mechanical, Maritime and Materials Engineering, Delft University of Technology, Leeghwaterstraat 39, 2628CB Delft, The Netherlands*

[3)]*Department of Physical, Chemical and Natural Systems, Universidad Pablo de Olavide, ES-41013 Sevilla, Spain*

[4)]*Department of Chemical and Biological Engineering, Northwestern University, 2145 Sheridan Road, Evanston, Illinois 60208, United States*

[5)]*Department of Applied Physics, Eindhoven University of Technology, 5600MB Eindhoven, The Netherlands*

(*Electronic mail: d.dubbeldam@uva.nl.)

(Dated: 28 August 2024)

[a)]https://www.uva.nl/profiel/d/u/d.dubbeldam/d.dubbeldam.html.

CONTENTS

S-I. BINARY PACKAGES

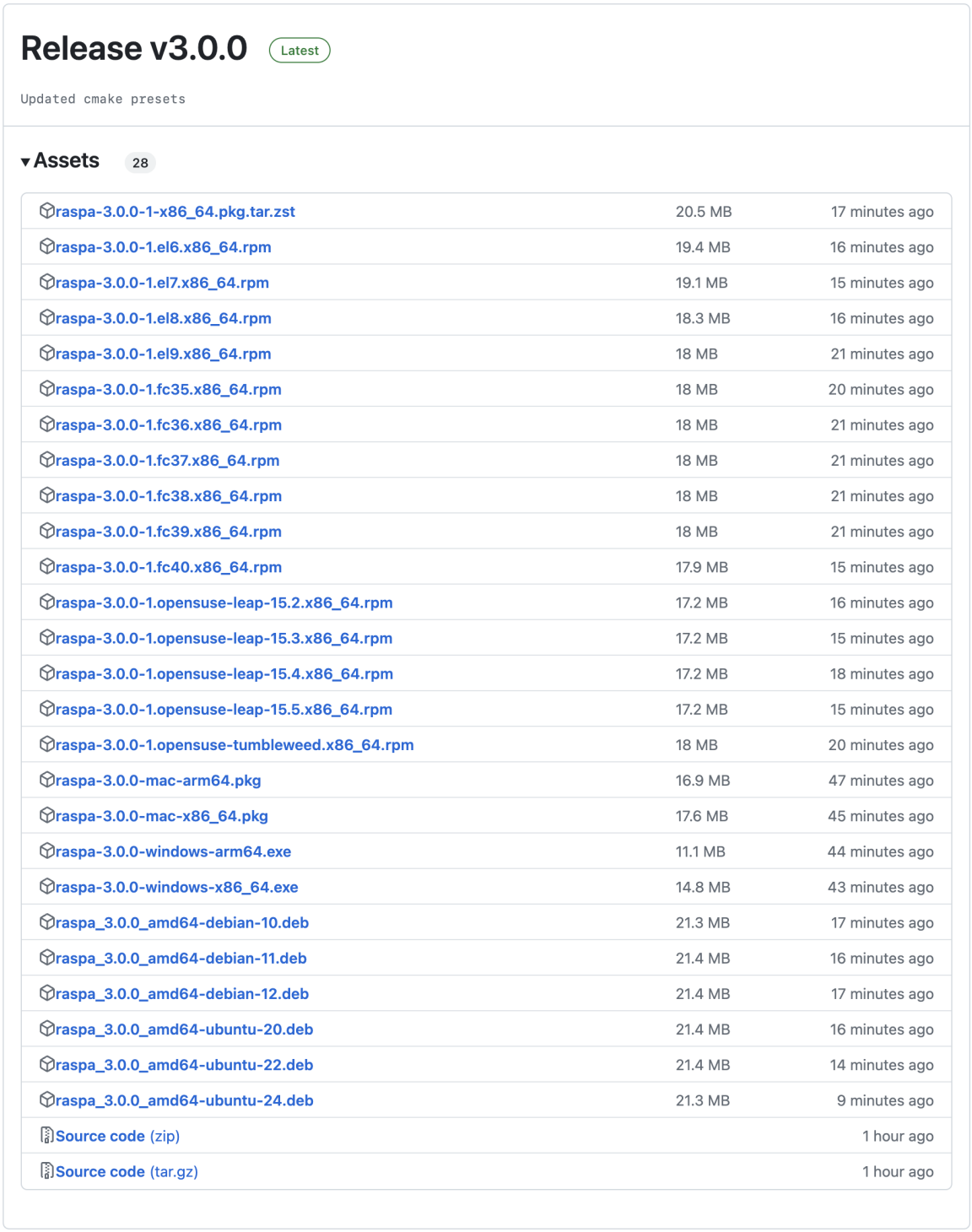

Release v3.0.0 Latest

Updated cmake presets

▾ **Assets** 28

raspa-3.0.0-1-x86_64.pkg.tar.zst	20.5 MB	17 minutes ago
raspa-3.0.0-1.el6.x86_64.rpm	19.4 MB	16 minutes ago
raspa-3.0.0-1.el7.x86_64.rpm	19.1 MB	15 minutes ago
raspa-3.0.0-1.el8.x86_64.rpm	18.3 MB	16 minutes ago
raspa-3.0.0-1.el9.x86_64.rpm	18 MB	21 minutes ago
raspa-3.0.0-1.fc35.x86_64.rpm	18 MB	20 minutes ago
raspa-3.0.0-1.fc36.x86_64.rpm	18 MB	21 minutes ago
raspa-3.0.0-1.fc37.x86_64.rpm	18 MB	21 minutes ago
raspa-3.0.0-1.fc38.x86_64.rpm	18 MB	21 minutes ago
raspa-3.0.0-1.fc39.x86_64.rpm	18 MB	21 minutes ago
raspa-3.0.0-1.fc40.x86_64.rpm	17.9 MB	15 minutes ago
raspa-3.0.0-1.opensuse-leap-15.2.x86_64.rpm	17.2 MB	16 minutes ago
raspa-3.0.0-1.opensuse-leap-15.3.x86_64.rpm	17.2 MB	15 minutes ago
raspa-3.0.0-1.opensuse-leap-15.4.x86_64.rpm	17.2 MB	18 minutes ago
raspa-3.0.0-1.opensuse-leap-15.5.x86_64.rpm	17.2 MB	15 minutes ago
raspa-3.0.0-1.opensuse-tumbleweed.x86_64.rpm	18 MB	20 minutes ago
raspa-3.0.0-mac-arm64.pkg	16.9 MB	47 minutes ago
raspa-3.0.0-mac-x86_64.pkg	17.6 MB	45 minutes ago
raspa-3.0.0-windows-arm64.exe	11.1 MB	44 minutes ago
raspa-3.0.0-windows-x86_64.exe	14.8 MB	43 minutes ago
raspa_3.0.0_amd64-debian-10.deb	21.3 MB	17 minutes ago
raspa_3.0.0_amd64-debian-11.deb	21.4 MB	16 minutes ago
raspa_3.0.0_amd64-debian-12.deb	21.4 MB	17 minutes ago
raspa_3.0.0_amd64-ubuntu-20.deb	21.4 MB	16 minutes ago
raspa_3.0.0_amd64-ubuntu-22.deb	21.4 MB	14 minutes ago
raspa_3.0.0_amd64-ubuntu-24.deb	21.3 MB	9 minutes ago
Source code (zip)		1 hour ago
Source code (tar.gz)		1 hour ago

FIG. S1: List of available binary packages: Linux distributions based on Red Hat and OpenSUSE (rpm-packages), Debian (deb-packages), and Arch Linux (tar.zst packages), installers for x64- and apple-silicon macs, and installers for windows x64- and arm64-computers.

S-II. NIST COMPARISON

Reference Calculations of Intermolecular Energy for SPC/E[1]

Configuration	1	2	3	4
N	400	300	200	100
Cell Lengths	$[30,30,30]$	$[27,30,36]$	$[30,30,30]$	$[36,36,36]$
Cell angles	$[100^\circ,95^\circ,75^\circ]$	$[90^\circ,75^\circ,90^\circ]$	$[85^\circ,75^\circ,80^\circ]$	$[90^\circ,60^\circ,90^\circ]$
Number of wave vectors	831	1068	838	1027
$E\text{disp}/k_B$ [K]	$1.11992\cdot10^5$	$4.32860\cdot10^4$	$1.44033\cdot10^4$	$2.50251\cdot10^4$
E_{LRC}/k_B [K]	$-4.10919\cdot10^3$	$-2.10561\cdot10^3$	$-1.02730\cdot10^3$	$-1.63091\cdot10^2$
$E\text{real}/k_B$ [K]	$-7.27219\cdot10^5$	$-4.76902\cdot10^5$	$-2.97129\cdot10^5$	$-1.71462\cdot10^5$
$E\text{fourier}/k_B$ [K]	$4.46770\cdot10^4$	$4.44094\cdot10^4$	$2.88974\cdot10^4$	$2.23372\cdot10^4$
E_{self}/k_B [K]	$-1.15820\cdot10^7$	$-8.68647\cdot10^6$	$-5.79098\cdot10^6$	$-2.89549\cdot10^6$
E_{intra}/k_B [K]	$1.14354\cdot10^7$	$8.57652\cdot10^6$	$5.71768\cdot10^6$	$2.85884\cdot10^6$
E_{total}/k_B [K]	$-7.21254\cdot10^5$	$-5.01259\cdot10^5$	$-3.28153\cdot10^5$	$-1.60912\cdot10^5$

RASPA3 Calculations of Intermolecular Energy for SPC/E

Configuration	1	2	3	4
N	400	300	200	100
Cell Lengths	$[30,30,30]$	$[27,30,36]$	$[30,30,30]$	$[36,36,36]$
Cell angles	$[100^\circ,95^\circ,75^\circ]$	$[90^\circ,75^\circ,90^\circ]$	$[85^\circ,75^\circ,80^\circ]$	$[90^\circ,60^\circ,90^\circ]$
Number of wave vectors	831	1068	838	1027
$E\text{disp}/k_B$ [K]	$1.11992\cdot10^5$	$4.32860\cdot10^4$	$1.44033\cdot10^4$	$2.50251\cdot10^4$
E_{LRC}/k_B [K]	$-4.10919\cdot10^3$	$-2.10561\cdot10^3$	$-1.02730\cdot10^3$	$-1.63091\cdot10^2$
$E\text{real}/k_B$ [K]	$-7.27219\cdot10^5$	$-4.76902\cdot10^5$	$-2.97129\cdot10^5$	$-1.71462\cdot10^5$
$E\text{fourier}/k_B$ [K]	$4.46770\cdot10^4$	$4.44094\cdot10^4$	$2.88974\cdot10^4$	$2.23372\cdot10^4$
E_{self}/k_B [K]	$-1.15820\cdot10^7$	$-8.68647\cdot10^6$	$-5.79098\cdot10^6$	$-2.89549\cdot10^6$
E_{intra}/k_B [K]	$1.14354\cdot10^7$	$8.57652\cdot10^6$	$5.71768\cdot10^6$	$2.85884\cdot10^6$
E_{total}/k_B [K]	$-7.21254\cdot10^5$	$-5.01259\cdot10^5$	$-3.28153\cdot10^5$	$-1.60912\cdot10^5$

TABLE S1: RASPA3 compared to NIST SPC/E Water Reference Calculations - Non-cuboid Cell - 10Å cutoff.

S-III. PYTHON

```python
import raspa
import numpy as np

# load example force field
ff = raspa.ForceField.exampleMoleculeForceField(useCharge=False)

# load example methane
mcmoves = raspa.MCMoveProbabilitiesParticles(probabilityTranslationMove=1.0)
methane = raspa.Component.exampleCH4(0, ff, particleProbabilities=mcmoves)

# initialize system
box = raspa.SimulationBox(30.0 * np.ones(3))
system = raspa.System(
    systemId=0,
    temperature=300.0,
    forceField=ff,
    components=[methane],
    initialNumberOfMolecules=[100],
    simulationBox=box,
    sampleMoviesEvery=10,
)

# initialize simulation
mc = raspa.MonteCarlo(
    numberOfCycles=10000,
    numberOfInitializationCycles=1000,
    systems=[system],
)

mc.run()
```

FIG. S2: Example python-input for a simple simulation of a box of methane.

S-IV. SIMULATION SETTINGS

All simulations are carried out on a AMD EPYC 7713 64-core processor as single-core jobs. For the RASPA3 comparison with RASPA2, we use versions `3.0.0` and `2.0.50` respectively. We use the example force fields shipped with RASPA2 and RASPA3 with parameters from references[2–7], unless specified otherwise. We run simulations for 1,000,000 production cycles, ensuring good statistics, sampling observables every cycle. All Monte Carlo move probabilities are done in equal ratio. For adsorption simulations, we use various insertion/deletion schemes: the conventional swap (unbiased random insertion), Configuration-Biased Monte Carlo (CBMC) with 10 trial locations/directions, Continuous Fractional Component Monte Carlo (CFCMC), and a hybrid of the latter two schemes (CB/CFCMC). For CBMC we use 10 trial directions and for CFCMC we use 41 λ sampling points. For molecules with partial charges (CO_2 and N_2), we use the conventional Ewald summation with a relative precision of 10^{-6}.

S-V. ADSORPTION SIMULATION OF METHANE IN $2 \times 2 \times 2$ MFI AT 300K

Simulation phase	Duration / cycles
Initialization cycles	250000
Equilibration cycles	250000
Production cycles	1000000

atom	ε/k_B / K	σ / Å	charge / e	mass / amu
O	53.0	3.30	-1.025	15.9994
Si	22.0	2.30	2.05	28.0855
CH_4	158.5	3.72	-	16.04246

TABLE S2: Force field for CH_4 in $2 \times 2 \times 2$ MFI at 300K. The zeolite atoms are modeled using the TraPPE-zeo force field[3]. The CH_4 is modeled using the united-atom approach, and has been taken from Martin et al.[4]. Cross terms are computed using the Lorentz-Berthelot mixing rules. The VDW interactions are neglected beyond the cutoff of 12 Å, and the potential is shifted to zero at the cutoff (i.e. no tail-corrections are applied). The Ewald charge computation has been omitted, since CH_4 is neutral. The positions for the MFI atoms have been taken from Van Koningsveld[8] and the structure has been kept rigid.

Version	Fugacity, f / Pa	Absolute loading / molecules cell^{-1}			
		Conventional MC	CBMC	CFCMC	CB/CFCMC
RASPA2	10^3	-	0.0353 ± 0.0001	0.0351 ± 0.0009	0.0350 ± 0.0005
RASPA3	10^3	0.0352 ± 0.0006	0.0354 ± 0.0003	0.0351 ± 0.0003	0.0351 ± 0.0002
RASPA2	10^4	-	0.3473 ± 0.0013	0.3447 ± 0.0056	0.3434 ± 0.0021
RASPA3	10^4	0.3448 ± 0.0037	0.3465 ± 0.0021	0.3442 ± 0.0072	0.3435 ± 0.0044
RASPA2	10^5	-	2.8952 ± 0.0088	2.8701 ± 0.0330	2.8656 ± 0.0115
RASPA3	10^5	2.8891 ± 0.0284	2.8882 ± 0.0143	2.8413 ± 0.0515	2.8663 ± 0.0093
RASPA2	10^6	-	10.9500 ± 0.0083	10.8702 ± 0.0345	10.8861 ± 0.0159
RASPA3	10^6	10.9600 ± 0.0342	10.9504 ± 0.0128	10.8224 ± 0.0437	10.8922 ± 0.0166
RASPA2	10^7	-	16.1028 ± 0.0102	16.0207 ± 0.0727	16.0181 ± 0.0116
RASPA3	10^7	16.1130 ± 0.0286	16.1023 ± 0.0101	16.0390 ± 0.0277	16.0206 ± 0.0212
RASPA2	10^8	-	18.3976 ± 0.0065	18.3715 ± 0.0742	18.3747 ± 0.0279
RASPA3	10^8	18.4089 ± 0.0497	18.3929 ± 0.0197	18.3336 ± 0.0263	18.3107 ± 0.0189
RASPA2	10^9	-	20.2099 ± 0.0347	20.1825 ± 0.0553	20.1541 ± 0.0246
RASPA3	10^9	20.2553 ± 0.0646	20.2045 ± 0.0446	20.1410 ± 0.1014	20.1348 ± 0.0296
RASPA2	10^{10}	-	21.5513 ± 0.0386	21.5647 ± 0.0688	21.5686 ± 0.0460
RASPA3	10^{10}	21.5990 ± 0.1000	21.5639 ± 0.0381	21.4603 ± 0.0930	21.4806 ± 0.0161
RASPA2	10^{11}	-	22.4903 ± 0.0564	22.5156 ± 0.0698	22.4637 ± 0.0517
RASPA3	10^{11}	22.4334 ± 0.0560	22.4627 ± 0.0321	22.3678 ± 0.1514	22.3782 ± 0.0301
RASPA2	10^{12}	-	22.9930 ± 0.0262	23.0257 ± 0.0419	22.9833 ± 0.0680
RASPA3	10^{12}	23.0077 ± 0.0685	22.9942 ± 0.0138	22.9088 ± 0.0582	22.9332 ± 0.0241

TABLE S3: Loading of methane in $2 \times 2 \times 2$ MFI at 300K for different insertion methods and code versions.

f / Pa		μ_N	Bins											
	N		0	1	2	3	4							
10^3	RASPA2	0.28	751	218	28	2	1							
	RASPA3	0.28	751	217	31	1	0							
	N		0	1	2	3	4	5	6	7	8	9	10	11
10^4	RASPA2	2.83	53	178	224	221	155	113	41	11	3	0	0	1
	RASPA3	2.80	47	188	233	232	156	79	38	19	4	3	1	0
	N		7-9	10-12	13-15	16-18	19-21	22-24	25-27	28-30	31-33	34-36	37-39	40-42
10^5	RASPA2	22.86	1	6	32	132	221	269	174	126	30	6	3	0
	RASPA3	22.81	1	6	35	111	252	257	192	109	26	10	0	1
	N		67-70	71-74	75-78	79-82	83-86	87-90	91-94	95-98	99-102	103-106		
10^6	RASPA2	87.27	2	10	39	127	255	299	179	73	13	3		
	RASPA3	87.23	0	7	34	146	264	286	180	73	9	1		
	N		116-117	118-119	120-121	122-123	124-125	126-127	128-129	130-131	132-133	134-135	136-137	138-139
10^7	RASPA2	128.02	0	3	24	50	145	213	251	167	105	33	6	3
	RASPA3	128.07	2	8	17	66	135	201	229	181	116	31	14	0
	N		137-138	139-140	141-142	143-144	145-146	147-148	149-150	151-152	153-154	155-156		
10^8	RASPA2	146.67	3	8	38	152	268	296	173	53	9	0		
	RASPA3	146.42	0	7	61	156	299	279	134	55	7	2		
	N		152-153	154-155	156-157	158-159	160-161	162-163	164-165	166-167	168-169	170-171		
10^9	RASPA2	160.66	3	11	76	216	322	268	92	9	3	0		
	RASPA3	161.01	2	11	63	201	301	261	135	24	0	2		
	N		164-165	166-167	168-169	170-171	172-173	174-175	176-177	178-179				
10^{10}	RASPA2	172.01	0	11	89	276	408	193	20	3				
	RASPA3	171.76	1	8	119	329	357	156	29	1				
	N		172-173	174-175	176-177	178-179	180-181	182-183	184-185					
10^{11}	RASPA2	179.17	0	20	147	397	351	84	1					
	RASPA3	178.93	1	16	185	417	340	41	0					
	N		179	180	181	182	183	184	185	186	187	188		
10^{12}	RASPA2	183.39	2	17	39	144	348	285	119	36	9	1		
	RASPA3	183.38	0	3	51	152	359	267	133	31	4	0		

TABLE S4: Particle number distribution for methane in $2 \times 2 \times 2$ MFI at 300K for the CB/CFCMC insertion method.

Version	Fugacity, f / Pa	Simulation time / hh:mm			
		Conventional MC	CBMC	CFCMC	CB/CFCMC
RASPA2	10^3	-	1:55	2:34	2:52
RASPA3	10^3	0:18	0:25	0:37	0:43
RASPA2	10^4	-	3:07	2:39	3:05
RASPA3	10^4	0:32	0:42	0:37	0:44
RASPA2	10^5	-	3:55	3:18	3:52
RASPA3	10^5	0:39	0:51	0:44	0:53
RASPA2	10^6	-	14:14	11:51	13:39
RASPA3	10^6	2:10	2:56	2:27	3:04
RASPA2	10^7	-	21:45	17:30	19:21
RASPA3	10^7	3:03	4:01	3:27	4:13
RASPA2	10^8	-	25:34	20:05	22:12
RASPA3	10^8	3:24	4:28	3:53	4:41
RASPA2	10^9	-	28:31	22:22	24:22
RASPA3	10^9	3:38	4:48	4:10	5:03
RASPA2	10^{10}	-	30:23	23:51	26:01
RASPA3	10^{10}	3:51	5:03	4:24	5:24
RASPA2	10^{11}	-	31:50	25:18	26:58
RASPA3	10^{11}	3:57	5:13	4:34	5:34
RASPA2	10^{12}	-	33:04	25:47	27:37
RASPA3	10^{12}	4:01	5:18	4:38	5:41
RASPA2	Total	-	194:19	155:16	169:59
RASPA3	Total	25:33	33:45	29:32	36:02

TABLE S5: Simulation time of the GCMC simulation of methane in $2 \times 2 \times 2$ MFI at 300K for different insertion methods and code versions.

Version	Fugacity, f / Pa	Enthalpy of adsorption, H_{ads} / kJ mol^{-1}			
		Conventional MC	CBMC	CFCMC	CB/CFCMC
RASPA2	10^3	-	-19.002 ± 0.022	-19.066 ± 0.120	-19.021 ± 0.074
RASPA3	10^3	-19.004 ± 0.019	-19.001 ± 0.010	-19.014 ± 0.067	-19.002 ± 0.047
RASPA2	10^4	-	-19.032 ± 0.012	-19.039 ± 0.068	-19.017 ± 0.014
RASPA3	10^4	-19.027 ± 0.019	-19.032 ± 0.009	-19.019 ± 0.052	-19.025 ± 0.026
RASPA2	10^5	-	-19.268 ± 0.034	-19.282 ± 0.049	-19.290 ± 0.027
RASPA3	10^5	-19.248 ± 0.031	-19.257 ± 0.019	-19.262 ± 0.075	-19.246 ± 0.044
RASPA2	10^6	-	-20.170 ± 0.033	-20.150 ± 0.051	-20.152 ± 0.030
RASPA3	10^6	-20.199 ± 0.052	-20.187 ± 0.026	-20.121 ± 0.065	-20.139 ± 0.057
RASPA2	10^7	-	-19.782 ± 0.034	-19.181 ± 0.175	-19.302 ± 0.203
RASPA3	10^7	-19.943 ± 0.159	-19.817 ± 0.075	-19.549 ± 0.179	-19.626 ± 0.119
RASPA2	10^8	-	-16.761 ± 0.195	-16.201 ± 0.329	-16.249 ± 0.197
RASPA3	10^8	-16.801 ± 0.396	-16.881 ± 0.091	-16.546 ± 0.271	-16.533 ± 0.261
RASPA2	10^9	-	-14.182 ± 0.355	-14.113 ± 0.637	-13.863 ± 0.385
RASPA3	10^9	-14.104 ± 0.474	-14.065 ± 0.690	-13.761 ± 0.653	-13.533 ± 0.926
RASPA2	10^{10}	-	-10.414 ± 0.685	-10.011 ± 0.849	-9.431 ± 1.069
RASPA3	10^{10}	-9.400 ± 2.006	-10.165 ± 0.835	-9.791 ± 1.207	-9.544 ± 0.621
RASPA2	10^{11}	-	-4.348 ± 1.171	-3.999 ± 1.012	-4.633 ± 2.237
RASPA3	10^{11}	-4.149 ± 2.074	-4.090 ± 1.397	-2.993 ± 1.769	-3.364 ± 0.216
RASPA2	10^{12}	-	4.479 ± 1.977	5.154 ± 1.420	3.636 ± 1.738
RASPA3	10^{12}	5.093 ± 4.669	5.233 ± 0.957	3.411 ± 1.109	4.229 ± 1.525

TABLE S6: Enthalpy of adsorption of methane in $2 \times 2 \times 2$ MFI at 300K for different insertion methods and code versions.

Fugacity, f / Pa	Chemical potential, μ / kJ mol^{-1}				
	Widom	CFCMC		CB/CFCMC	
	$\left\langle e^{-\beta U^+} \right\rangle$	$\left\langle \ln \frac{P(\lambda=1)}{P(\lambda=0)} \right\rangle$	$\int \langle dU/d\lambda \rangle d\lambda$	$\left\langle \ln \frac{P(\lambda=1)}{P(\lambda=0)} \right\rangle$	$\int \langle dU/d\lambda \rangle d\lambda$
10^3	-37.995 ± 0.018	-38.014 ± 0.091	-38.078 ± 0.034	-38.027 ± 0.096	-38.065 ± 0.042
10^4	-32.263 ± 0.017	-32.274 ± 0.049	-32.303 ± 0.076	-32.251 ± 0.018	-32.341 ± 0.042
10^5	-26.584 ± 0.013	-26.560 ± 0.057	-26.627 ± 0.034	-26.559 ± 0.089	-26.639 ± 0.105
10^6	-20.785 ± 0.006	-20.770 ± 0.091	-20.807 ± 0.067	-20.783 ± 0.035	-20.829 ± 0.052
10^7	-15.020 ± 0.015	-14.986 ± 0.086	-14.885 ± 0.206	-15.048 ± 0.086	-14.937 ± 0.042
10^8	-9.289 ± 0.039	-9.271 ± 0.080	-9.113 ± 0.055	-9.303 ± 0.055	-9.120 ± 0.129
10^9	-3.665 ± 0.107	-3.538 ± 0.053	-3.436 ± 0.224	-3.556 ± 0.043	-3.430 ± 0.032
10^{10}	1.967 ± 0.122	2.170 ± 0.112	2.179 ± 0.152	2.240 ± 0.034	2.152 ± 0.111
10^{11}	7.527 ± 1.648	7.943 ± 0.055	7.856 ± 0.092	7.936 ± 0.076	7.836 ± 0.205
10^{12}	14.835 ± 3.632	13.667 ± 0.057	13.650 ± 0.074	13.676 ± 0.055	13.621 ± 0.071

TABLE S7: Excess chemical potential of methane in $2 \times 2 \times 2$ MFI at 300K for different insertion methods.

Fugacity, f / Pa	Measured fugacity, f/ Pa				
	Widom	CFCMC		CB/CFCMC	
	$\left\langle e^{-\beta U^+} \right\rangle$	$\left\langle \ln \frac{P(\lambda=1)}{P(\lambda=0)} \right\rangle$	$\int \langle dU/d\lambda \rangle d\lambda$	$\left\langle \ln \frac{P(\lambda=1)}{P(\lambda=0)} \right\rangle$	$\int \langle dU/d\lambda \rangle d\lambda$
10^3	$1.0 \cdot 10^3 \pm 7.4 \cdot 10^0$	$9.97 \cdot 10^2 \pm 3.62 \cdot 10^1$	$9.71 \cdot 10^2 \pm 1.33 \cdot 10^1$	$9.91 \cdot 10^2 \pm 3.82 \cdot 10^1$	$9.76 \cdot 10^2 \pm 1.65 \cdot 10^1$
10^4	$9.99 \cdot 10^3 \pm 6.8 \cdot 10^1$	$9.95 \cdot 10^3 \pm 1.95 \cdot 10^2$	$9.84 \cdot 10^3 \pm 3.02 \cdot 10^2$	$1.0 \cdot 10^4 \pm 7.44 \cdot 10^1$	$9.69 \cdot 10^3 \pm 1.64 \cdot 10^2$
10^5	$9.74 \cdot 10^4 \pm 5.11 \cdot 10^2$	$9.84 \cdot 10^4 \pm 2.24 \cdot 10^3$	$9.57 \cdot 10^4 \pm 1.3 \cdot 10^3$	$9.84 \cdot 10^4 \pm 3.47 \cdot 10^3$	$9.53 \cdot 10^4 \pm 4.05 \cdot 10^3$
10^6	$9.96 \cdot 10^5 \pm 2.5 \cdot 10^3$	$1.0 \cdot 10^6 \pm 3.65 \cdot 10^4$	$9.88 \cdot 10^5 \pm 2.68 \cdot 10^4$	$9.97 \cdot 10^5 \pm 1.4 \cdot 10^4$	$9.78 \cdot 10^5 \pm 2.02 \cdot 10^4$
10^7	$1.0 \cdot 10^7 \pm 6.14 \cdot 10^4$	$1.02 \cdot 10^7 \pm 3.5 \cdot 10^5$	$1.06 \cdot 10^7 \pm 8.68 \cdot 10^5$	$9.94 \cdot 10^6 \pm 3.41 \cdot 10^5$	$1.04 \cdot 10^7 \pm 1.73 \cdot 10^5$
10^8	$1.0 \cdot 10^8 \pm 1.54 \cdot 10^6$	$1.01 \cdot 10^8 \pm 3.2 \cdot 10^6$	$1.07 \cdot 10^8 \pm 2.37 \cdot 10^6$	$9.94 \cdot 10^7 \pm 2.18 \cdot 10^6$	$1.07 \cdot 10^8 \pm 5.49 \cdot 10^6$
10^9	$9.53 \cdot 10^8 \pm 4.0 \cdot 10^7$	$1.0 \cdot 10^9 \pm 2.14 \cdot 10^7$	$1.04 \cdot 10^9 \pm 9.39 \cdot 10^7$	$9.96 \cdot 10^8 \pm 1.72 \cdot 10^7$	$1.05 \cdot 10^9 \pm 1.36 \cdot 10^7$
10^{10}	$9.12 \cdot 10^9 \pm 4.4 \cdot 10^8$	$9.89 \cdot 10^9 \pm 4.44 \cdot 10^8$	$9.92 \cdot 10^9 \pm 6.0 \cdot 10^8$	$1.02 \cdot 10^{10} \pm 1.38 \cdot 10^8$	$9.81 \cdot 10^9 \pm 4.36 \cdot 10^8$
10^{11}	$8.47 \cdot 10^{10} \pm 7.8 \cdot 10^{10}$	$1.0 \cdot 10^{11} \pm 2.19 \cdot 10^9$	$9.66 \cdot 10^{10} \pm 3.6 \cdot 10^9$	$9.98 \cdot 10^{10} \pm 3.02 \cdot 10^9$	$9.58 \cdot 10^{10} \pm 8.16 \cdot 10^9$
10^{12}	$1.59 \cdot 10^{12} \pm 4.31 \cdot 10^{12}$	$9.92 \cdot 10^{11} \pm 2.28 \cdot 10^{10}$	$9.86 \cdot 10^{11} \pm 2.91 \cdot 10^{10}$	$9.96 \cdot 10^{11} \pm 2.21 \cdot 10^{10}$	$9.74 \cdot 10^{11} \pm 2.77 \cdot 10^{10}$

TABLE S8: Measured fugacity of methane in $2 \times 2 \times 2$ MFI at 300K for different insertion methods.

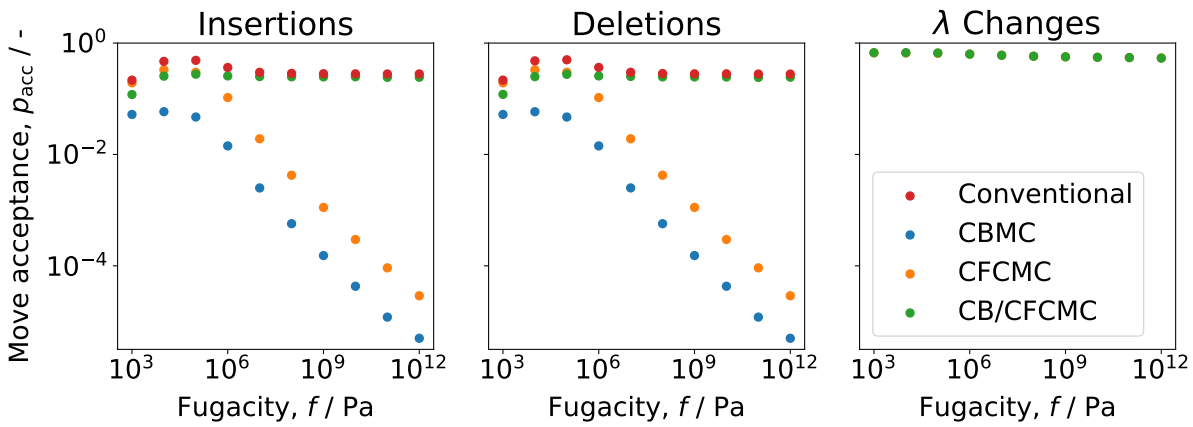

FIG. S3: Acceptance rate per attempted Monte-Carlo move for grand-canonical simulations of methane in $2 \times 2 \times 2$ MFI at 300K performed with conventional swap (red), CBMC (blue), CFCMC (orange) and CB/CFCMC (green).

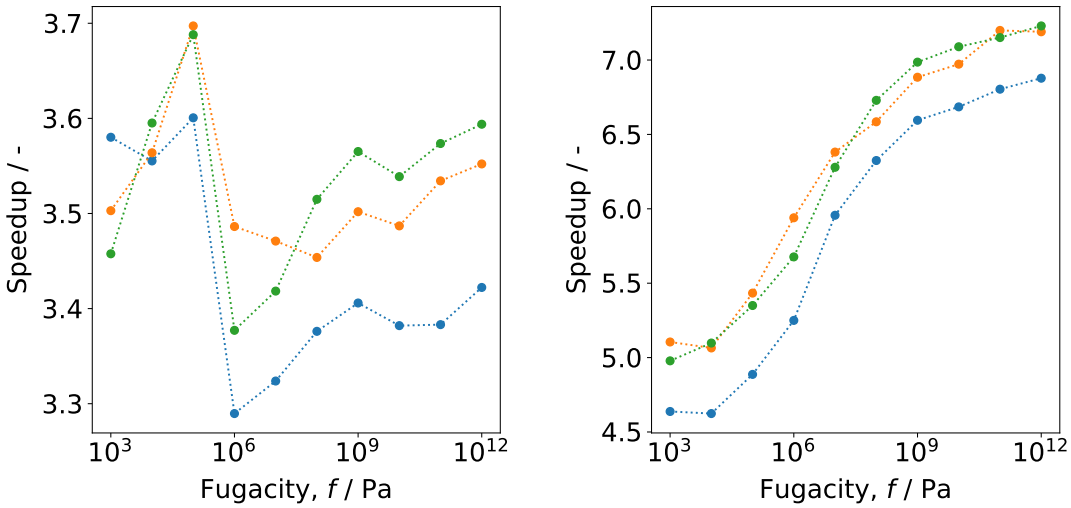

(a) Translation

(b) Widom

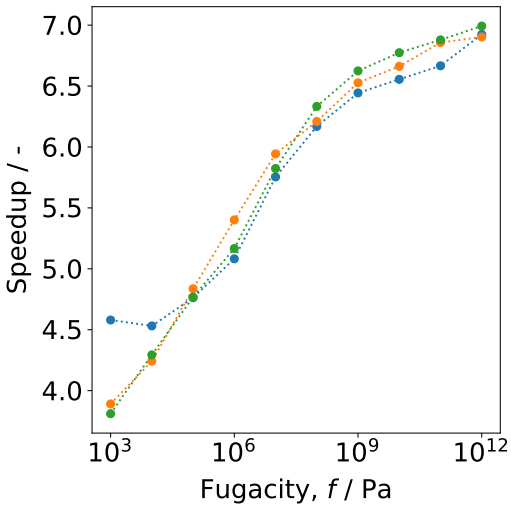

(c) Reinsertion (CBMC)

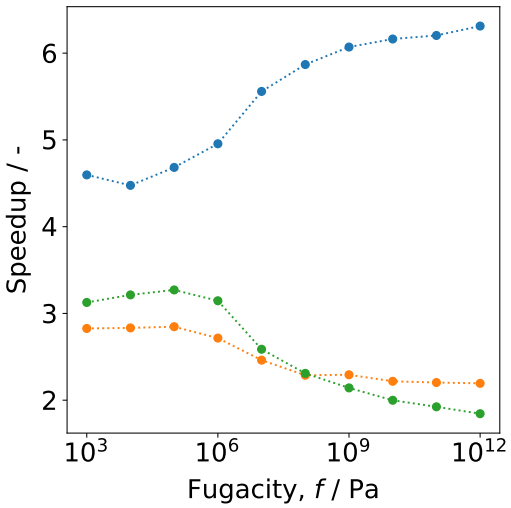

(d) Insertion

FIG. S4: Relative speedup of RASPA3 over RASPA2 evaluated per attempted Monte-Carlo move for grand-canonical simulations of methane in $2 \times 2 \times 2$ MFI at 300K performed with CBMC (blue), CFCMC (orange) and CB/CFCMC (green).

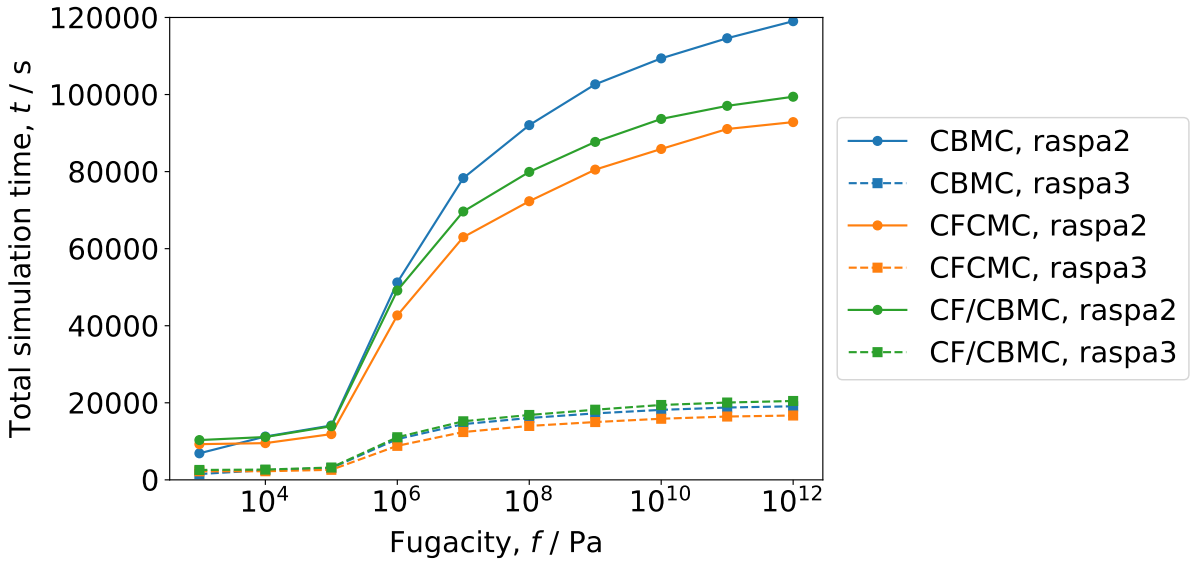

FIG. S5: Production simulation time per Grand-Canonical simulation of methane in $2 \times 2 \times 2$ MFI at 300K performed with CBMC (blue), CFCMC (orange) and CB/CFCMC (green).

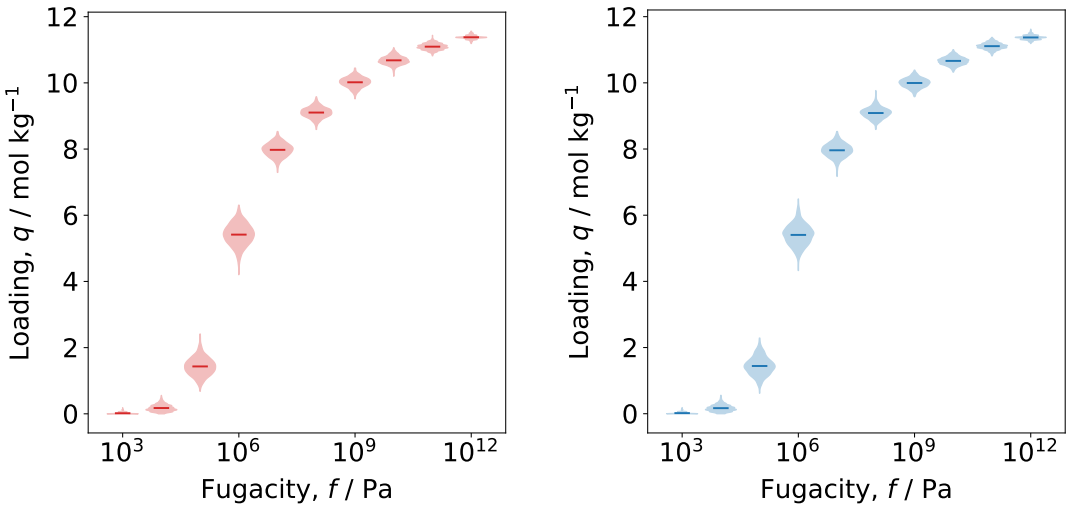

(a) Conventional

(b) CBMC

(c) CFCMC

(d) CB/CFCMC

FIG. S6: Particle distributions per Grand-Canonical adsorption simulation of methane in $2 \times 2 \times 2$ MFI at 300K performed with conventional swap (red), CBMC (blue), CFCMC (orange) and CB/CFCMC (green).

S-VI. ADSORPTION SIMULATION OF CO_2 IN $2 \times 2 \times 2$ MFI AT 300K

Simulation phase	Duration / cycles
Initialization cycles	500000
Equilibration cycles	500000
Production cycles	1000000

atom	ε/k_B / K	σ / Å	charge / e	mass / amu
O	53.0	3.30	-1.025	15.9994
Si	22.0	2.30	2.05	28.0855
O_{co2}	85.671	3.017	-0.3256	15.9994
C_{co2}	29.933	2.745	0.6512	12.0

TABLE S9: Force field for CO_2 in $2 \times 2 \times 2$ MFI at 300K. The zeolite atoms are modeled using the TraPPE-zeo force field[3]. The CO_2 model has bond-lengths of 1.149 Å, and has been taken from García-Sanchez et al.[7]. Cross terms are computed using the Lorentz-Berthelot mixing rules. The VDW interactions are neglected beyond the cutoff of 12 Å, and the potential is shifted to zero at the cutoff (i.e. no tail-corrections are applied). The Ewald precision is set to 10^{-6}. The positions for the MFI atoms have been taken from Van Koningsveld[8] and the structure has been kept rigid.

Version	Fugacity, f / Pa	Absolute loading / molecules $\cdot$ cell^{-1}			
		conventional MC	CBMC	CFCMC	CB/CFCMC
RASPA2	10^1	-	0.01630 ± 0.00040	0.01577 ± 0.00164	0.01581 ± 0.00168
RASPA3	10^1	0.01644 ± 0.00026	0.01626 ± 0.00031	0.01643 ± 0.00052	0.01636 ± 0.00032
RASPA2	10^2	-	0.1632 ± 0.0013	0.1611 ± 0.0062	0.1634 ± 0.0039
RASPA3	10^2	0.1609 ± 0.0016	0.1626 ± 0.0023	0.1626 ± 0.0027	0.1625 ± 0.0016
RASPA2	10^3	-	1.617 ± 0.002	1.602 ± 0.015	1.619 ± 0.024
RASPA3	10^3	1.605 ± 0.022	1.616 ± 0.006	1.600 ± 0.038	1.611 ± 0.022
RASPA2	10^4	-	14.86 ± 0.06	14.63 ± 0.19	14.69 ± 0.13
RASPA3	10^4	14.92 ± 0.20	14.86 ± 0.03	14.74 ± 0.23	14.73 ± 0.10
RASPA2	10^5	-	75.62 ± 0.13	74.63 ± 0.41	75.04 ± 0.24
RASPA3	10^5	75.61 ± 0.51	75.53 ± 0.06	74.93 ± 0.53	75.07 ± 0.26
RASPA2	10^6	-	128.41 ± 0.09	127.32 ± 0.54	127.52 ± 0.09
RASPA3	10^6	128.20 ± 0.20	128.38 ± 0.11	127.41 ± 1.11	127.56 ± 0.12
RASPA2	10^7	-	153.84 ± 0.20	153.31 ± 0.53	153.33 ± 0.26
RASPA3	10^7	153.43 ± 0.47	153.93 ± 0.27	153.79 ± 0.66	152.93 ± 0.27
RASPA2	10^8	-	169.66 ± 0.43	169.32 ± 0.32	169.76 ± 0.31
RASPA3	10^8	170.01 ± 0.35	169.76 ± 0.37	168.79 ± 0.64	168.90 ± 0.63
RASPA2	10^9	-	179.91 ± 0.35	179.57 ± 0.46	179.49 ± 0.43
RASPA3	10^9	179.58 ± 1.51	179.59 ± 0.32	178.84 ± 1.45	179.19 ± 0.71
RASPA2	10^{10}	-	190.10 ± 0.31	190.45 ± 2.05	189.72 ± 0.84
RASPA3	10^{10}	189.83 ± 2.03	189.78 ± 0.50	189.94 ± 1.48	189.65 ± 1.00

TABLE S10: Absolute loading of CO_2 in $2 \times 2 \times 2$ MFI at 300K.

Version	Fugacity, f / Pa	Enthalpy of adsorption, H_{ads} / kJ $\cdot$ mol^{-1}			
		conventional MC	CBMC	CFCMC	CB/CFCMC
RASPA2	10^1	-	-26.96 ± 0.09	-26.72 ± 0.91	-26.76 ± 0.74
RASPA3	10^1	-26.87 ± 0.10	-26.94 ± 0.06	-26.95 ± 0.41	-26.94 ± 0.39
RASPA2	10^2	-	-26.96 ± 0.02	-26.90 ± 0.20	-27.05 ± 0.40
RASPA3	10^2	-26.91 ± 0.03	-26.97 ± 0.03	-26.97 ± 0.09	-26.98 ± 0.12
RASPA2	10^3	-	-26.96 ± 0.02	-27.00 ± 0.12	-26.99 ± 0.12
RASPA3	10^3	-26.96 ± 0.03	-27.01 ± 0.02	-27.01 ± 0.02	-26.94 ± 0.05
RASPA2	10^4	-	-27.12 ± 0.03	-27.13 ± 0.08	-27.11 ± 0.04
RASPA3	10^4	-27.10 ± 0.05	-27.09 ± 0.04	-27.11 ± 0.06	-27.10 ± 0.06
RASPA2	10^5	-	-28.47 ± 0.08	-28.55 ± 0.13	-28.55 ± 0.11
RASPA3	10^5	-28.47 ± 0.08	-28.48 ± 0.08	-28.45 ± 0.13	-28.43 ± 0.09
RASPA2	10^6	-	-30.82 ± 0.27	-30.59 ± 0.31	-30.54 ± 0.12
RASPA3	10^6	-30.54 ± 0.39	-30.56 ± 0.25	-30.25 ± 0.57	-30.58 ± 0.29
RASPA2	10^7	-	-31.00 ± 0.70	-29.13 ± 0.81	-29.18 ± 1.40
RASPA3	10^7	-31.32 ± 0.68	-31.12 ± 0.58	-30.26 ± 0.60	-30.07 ± 0.80
RASPA2	10^8	-	-28.31 ± 0.72	-28.40 ± 1.35	-27.14 ± 1.16
RASPA3	10^8	-26.90 ± 2.62	-27.81 ± 0.92	-26.91 ± 1.27	-27.13 ± 0.64
RASPA2	10^9	-	-21.09 ± 0.99	-19.95 ± 2.97	-21.52 ± 0.42
RASPA3	10^9	-20.79 ± 2.69	-21.67 ± 1.18	-20.86 ± 1.13	-20.47 ± 1.26
RASPA2	10^{10}	-	-16.96 ± 2.09	-17.32 ± 1.93	-16.50 ± 2.41
RASPA3	10^{10}	-16.98 ± 4.01	-16.46 ± 2.02	-14.63 ± 2.42	-16.98 ± 4.01

TABLE S11: Enthalpy of adsorption of CO2 in $2 \times 2 \times 2$ MFI at 300K.

Version	Fugacity, f / Pa	Acceptance percentages / %					Total accepted / -	
		translation	rotation	reinsertion	insertion	deletion	insertion	deletion
RASPA2	10^1	55.98	50.61	17.67	1.61	1.61	64302	64302
RASPA3	10^1	51.05	51.17	20.29	1.60	1.60	63870	63870
RASPA2	10^2	55.90	50.15	17.22	10.81	10.79	432003	432003
RASPA3	10^2	50.29	50.28	19.97	11.04	11.04	441401	441401
RASPA2	10^3	55.92	49.99	17.22	27.62	27.63	1104680	1104681
RASPA3	10^3	50.01	50.09	19.98	29.33	29.31	1173123	1173118
RASPA2	10^4	55.17	50.01	15.54	30.00	29.97	1208395	1208400
RASPA3	10^4	50.18	50.07	17.97	32.21	32.17	1296718	1296716
RASPA2	10^5	50.53	50.08	6.297	17.258	17.257	2609904	2609906
RASPA3	10^5	50.04	50.07	7.176	18.405	18.405	2780085	2780102
RASPA2	10^6	50.08	50.04	0.758	3.341	3.342	858115	858111
RASPA3	10^6	50.00	50.11	0.835	3.404	3.403	873972	873970
RASPA2	10^7	50.03	49.96	0.116	0.5622	0.5623	172987	172981
RASPA3	10^7	49.98	50.11	0.125	0.5642	0.5642	173718	173716
RASPA2	10^8	49.99	50.09	0.039	0.1049	0.1050	35606	35609
RASPA3	10^8	50.02	50.01	0.041	0.1064	0.1064	36116	36113
RASPA2	10^9	50.06	49.98	0.0243	0.0260	0.0260	9351	9352
RASPA3	10^9	50.02	50.00	0.0260	0.0253	0.0253	9076	9071
RASPA2	10^{10}	49.95	49.99	0.0181	0.0103	0.0103	3927	3921
RASPA3	10^{10}	50.04	50.04	0.0189	0.0102	0.0101	3853	3847

TABLE S12: Acceptance percentages of CBMC adsorption of CO2 in $2 \times 2 \times 2$ MFI at 300K.

Version	Fugacity, f / Pa	Acceptance percentages / %				Total accepted / -	
		reinsertion	λ-move	λ-insertion	λ-deletion	λ-insertion	λ-deletion
RASPA2	10^1	51.89	55.15	1.4257	1.4211	28325	28325
RASPA3	10^1	44.79	54.29	1.3355	1.3455	26161	26161
RASPA2	10^2	49.55	55.04	7.0574	6.9817	140455	140455
RASPA3	10^2	43.16	54.23	6.7285	6.7837	131798	131799
RASPA2	10^3	34.43	54.87	13.7519	13.7702	275276	275276
RASPA3	10^3	32.60	54.02	17.4182	17.1449	334927	334926
RASPA2	10^4	17.72	54.11	14.5692	14.5848	292589	292583
RASPA3	10^4	19.52	53.76	19.2952	19.2287	380156	380152
RASPA2	10^5	6.66	50.03	15.1752	15.1026	941059	941058
RASPA3	10^5	7.38	51.34	17.5691	17.6480	1305690	1305696
RASPA2	10^6	0.922	50.05	21.87055	22.3270	1558399	1558407
RASPA3	10^6	0.9691	49.96	22.8828	22.9847	2341055	2341049
RASPA2	10^7	0.231	50.08	27.1910	26.4462	1794893	1794894
RASPA3	10^7	0.225	50.00	27.1020	27.2669	2918861	2918860
RASPA2	10^8	0.145	50.07	30.1347	30.5711	2004421	2004423
RASPA3	10^8	0.141	49.96	30.2981	29.6312	3205924	3205920
RASPA2	10^9	0.120	50.00	32.6239	33.5260	1942758	1942759
RASPA3	10^9	0.113	50.00	30.5353	30.9538	3310238	3310237
RASPA2	10^{10}	0.110	50.10	34.5362	34.2989	1995449	1995444
RASPA3	10^{10}	0.093	50.08	32.5925	31.6542	3231317	3231317

TABLE S13: Acceptance percentages of CFCMC adsorption of CO2 in $2 \times 2 \times 2$ MFI at 300K.

Version	Fugacity, f / Pa	Acceptance percentages / %				Total accepted / -	
		Reinsertion	λ-move	λ-insertion	λ-deletion	λ-insertion	λ-deletion
RASPA2	10^1	51.76	54.97	1.5823	1.5960	31789	31789
RASPA3	10^1	44.78	54.43	1.5867	1.6116	30985	30985
RASPA2	10^2	49.17	55.01	12.5115	12.7242	252427	252427
RASPA3	10^2	43.39	54.09	13.4128	13.3617	260864	260865
RASPA2	10^3	34.21	54.98	36.9087	37.4756	743284	743287
RASPA3	10^3	32.24	54.17	40.0002	40.1960	782037	782036
RASPA2	10^4	17.65	54.14	41.6994	41.7316	844183	844186
RASPA3	10^4	19.48	53.73	45.3565	45.1337	891397	891396
RASPA2	10^5	6.59	49.96	38.0147	38.3830	2413932	2413921
RASPA3	10^5	7.36	51.31	33.9699	33.8951	2517918	2517914
RASPA2	10^6	0.91	49.95	42.0380	42.6270	3007936	3007930
RASPA3	10^6	0.96	49.96	29.3533	29.2327	2983401	2983410
RASPA2	10^7	0.223	49.95	47.9136	49.1632	3349145	3349148
RASPA3	10^7	0.233	50.16	31.5281	31.7006	3342412	3342414
RASPA2	10^8	0.142	50.00	53.3459	54.3437	3519039	3519035
RASPA3	10^8	0.143	49.95	34.2113	34.1863	3690511	3690510
RASPA2	10^9	0.130	49.97	58.4483	57.4522	3694058	3694057
RASPA3	10^9	0.122	49.98	38.0523	36.7847	3929522	3929524
RASPA2	10^{10}	0.116	50.01	61.3798	58.7136	3567788	3567787
RASPA3	10^{10}	0.100	49.99	37.0909	36.7698	3820453	3820453

TABLE S14: Acceptance percentages of CB/CFCMC adsorption of CO2 in $2 \times 2 \times 2$ MFI at 300K.

Fugacity, f / Pa	Measured fugacity, f / Pa				
	Widom	CFCMC		CB/CFCMC	
	$\left\langle e^{-\beta U^+} \right\rangle$	$\left\langle \ln \frac{P(\lambda=1)}{P(\lambda=0)} \right\rangle$	$\int \langle \mathrm{d}U/\mathrm{d}\lambda \rangle \mathrm{d}\lambda$	$\left\langle \ln \frac{P(\lambda=1)}{P(\lambda=0)} \right\rangle$	$\int \langle \mathrm{d}U/\mathrm{d}\lambda \rangle \mathrm{d}\lambda$
10^1	$1.002 \cdot 10^1 \pm 0.021 \cdot 10^1$	$0.996 \cdot 10^1 \pm 0.046 \cdot 10^1$	$1.001 \cdot 10^1 \pm 0.028 \cdot 10^1$	$0.981 \cdot 10^1 \pm 0.048 \cdot 10^1$	$0.994 \cdot 10^1 \pm 0.023 \cdot 10^1$
10^2	$0.996 \cdot 10^2 \pm 0.004 \cdot 10^2$	$0.994 \cdot 10^2 \pm 0.035 \cdot 10^2$	$1.033 \cdot 10^2 \pm 0.026 \cdot 10^2$	$0.982 \cdot 10^2 \pm 0.044 \cdot 10^2$	$0.998 \cdot 10^2 \pm 0.048 \cdot 10^2$
10^3	$1.004 \cdot 10^3 \pm 0.028 \cdot 10^3$	$1.000 \cdot 10^3 \pm 0.010 \cdot 10^3$	$0.990 \cdot 10^3 \pm 0.027 \cdot 10^3$	$0.983 \cdot 10^3 \pm 0.034 \cdot 10^3$	$0.991 \cdot 10^3 \pm 0.027 \cdot 10^3$
10^4	$0.997 \cdot 10^4 \pm 0.003 \cdot 10^4$	$0.996 \cdot 10^4 \pm 0.021 \cdot 10^4$	$0.976 \cdot 10^4 \pm 0.016 \cdot 10^4$	$0.988 \cdot 10^4 \pm 0.010 \cdot 10^4$	$0.985 \cdot 10^4 \pm 0.022 \cdot 10^4$
10^5	$0.994 \cdot 10^5 \pm 0.007 \cdot 10^5$	$1.004 \cdot 10^5 \pm 0.033 \cdot 10^5$	$9.585 \cdot 10^5 \pm 0.036 \cdot 10^5$	$0.995 \cdot 10^5 \pm 0.011 \cdot 10^5$	$0.957 \cdot 10^5 \pm 0.036 \cdot 10^5$
10^6	$0.998 \cdot 10^6 \pm 0.018 \cdot 10^6$	$0.988 \cdot 10^6 \pm 0.034 \cdot 10^6$	$0.969 \cdot 10^6 \pm 0.038 \cdot 10^6$	$0.986 \cdot 10^6 \pm 0.026 \cdot 10^6$	$0.960 \cdot 10^6 \pm 0.027 \cdot 10^6$
10^7	$1.017 \cdot 10^7 \pm 0.020 \cdot 10^7$	$0.997 \cdot 10^7 \pm 0.030 \cdot 10^7$	$0.982 \cdot 10^7 \pm 0.064 \cdot 10^7$	$0.989 \cdot 10^7 \pm 0.034 \cdot 10^7$	$1.023 \cdot 10^7 \pm 0.051 \cdot 10^7$
10^8	$1.033 \cdot 10^8 \pm 0.057 \cdot 10^8$	$0.993 \cdot 10^8 \pm 0.040 \cdot 10^8$	$1.010 \cdot 10^8 \pm 0.030 \cdot 10^8$	$0.999 \cdot 10^8 \pm 0.017 \cdot 10^8$	$1.031 \cdot 10^8 \pm 0.029 \cdot 10^8$
10^9	$1.093 \cdot 10^9 \pm 0.368 \cdot 10^9$	$1.011 \cdot 10^9 \pm 0.017 \cdot 10^9$	$1.056 \cdot 10^9 \pm 0.090 \cdot 10^9$	$0.991 \cdot 10^9 \pm 0.025 \cdot 10^9$	$1.030 \cdot 10^9 \pm 0.032 \cdot 10^9$
10^{10}	$0.94 \cdot 10^{10} \pm 0.91 \cdot 10^{10}$	$1.00 \cdot 10^{10} \pm 0.04 \cdot 10^{10}$	$1.05 \cdot 10^{10} \pm 0.01 \cdot 10^{10}$	$0.99 \cdot 10^{10} \pm 0.04 \cdot 10^{10}$	$1.02 \cdot 10^{10} \pm 0.03 \cdot 10^{10}$

TABLE S15: Imposed fugacity vs. the measured fugacities for CO_2 in $2 \times 2 \times 2$ MFI at 300K computed with RASPA3.

S-VII. ADSORPTION SIMULATION OF CO_2/N_2 EQUIMOLAR MIXTURE IN $2 \times 2 \times 2$ MFI AT 300K

Simulation phase	Duration / cycles
Initialization cycles	500000
Equilibration cycles	500000
Production cycles	1000000

atom	ε/k_B / K	σ / Å	charge / e	mass / amu
O	53.0	3.30	-1.025	15.9994
Si	22.0	2.30	2.05	28.0855
O_{co2}	85.671	3.017	-0.3256	15.9994
C_{co2}	29.933	2.745	0.6512	12.0
N_{n2}	38.298	3.306	-0.405	14.00674
N_{com}	-	-	0.810	0.0

TABLE S16: Force field for CO_2 and N_2 in $2 \times 2 \times 2$ MFI at 300K. The zeolite atoms are modeled using the TraPPE-zeo force field[3]. The CO_2 model has bond-lengths of 1.149 Å, and has been taken from García-Sanchez et al.[7]. The N_2 model has bond-lengths of 0.55 Å, and has been taken from[5]. Cross terms are computed using the Lorentz-Berthelot mixing rules. The VDW interactions are neglected beyond the cutoff of 12 Å, and the potential is shifted to zero at the cutoff (i.e. no tail-corrections are applied). The Ewald precision is set to 10^{-6}. The positions for the MFI atoms have been taken from Van Koningsveld[8] and the structure has been kept rigid.

Version	Fugacity, f / Pa		Absolute loading / molecules $\cdot$ cell^{-1}			
			conventional MC	CBMC	CFCMC	CB/CFCMC
RASPA2	10^1	CO_2	-	0.0082 ± 0.0001	0.0082 ± 0.0013	0.0073 ± 0.0007
	10^1	N_2	-	0.0003 ± 0.0001	0.0003 ± 0.0002	0.0003 ± 0.0002
RASPA3	10^1	CO_2	0.0079 ± 0.0002	0.0082 ± 0.0002	0.0081 ± 0.0003	0.0080 ± 0.0002
	10^1	N_2	0.0004 ± 0.0001	0.0003 ± 0.0001	0.0003 ± 0.0006	0.0003 ± 0.0001
RASPA2	10^2	CO_2	-	0.0815 ± 0.0007	0.0817 ± 0.0015	0.0788 ± 0.0032
	10^2	N_2	-	0.0032 ± 0.0001	0.0033 ± 0.0006	0.0032 ± 0.0003
RASPA3	10^2	CO_2	0.0810 ± 0.0017	0.0816 ± 0.0009	0.0810 ± 0.0015	0.0793 ± 0.0012
	10^2	N_2	0.0032 ± 0.0001	0.0032 ± 0.0001	0.0031 ± 0.0003	0.0032 ± 0.0001
RASPA2	10^3	CO_2	-	0.8119 ± 0.0054	0.7995 ± 0.0160	0.8049 ± 0.0109
	10^3	N_2	-	0.0320 ± 0.0005	0.0326 ± 0.0017	0.0324 ± 0.0017
RASPA3	10^3	CO_2	0.8134 ± 0.0120	0.8106 ± 0.0045	0.8099 ± 0.0246	0.7979 ± 0.0051
	10^3	N_2	0.0325 ± 0.0005	0.0321 ± 0.0007	0.0312 ± 0.0011	0.0317 ± 0.0007
RASPA2	10^4	CO_2	-	7.7743 ± 0.0239	7.6531 ± 0.1050	7.7163 ± 0.0889
	10^4	N_2	-	0.3020 ± 0.0033	0.2996 ± 0.0073	0.2973 ± 0.0059
RASPA3	10^4	CO_2	7.7881 ± 0.0100	7.7990 ± 0.0362	7.6094 ± 0.1906	7.6726 ± 0.0520
	10^4	N_2	0.3036 ± 0.0021	0.3030 ± 0.0022	0.2987 ± 0.0058	0.2980 ± 0.0028
RASPA2	10^5	CO_2	-	51.642 ± 0.192	50.677 ± 0.559	50.861 ± 0.375
	10^5	N_2	-	1.8352 ± 0.0088	1.7839 ± 0.0181	1.7846 ± 0.0334
RASPA3	10^5	CO_2	51.595 ± 0.2761	51.716 ± 0.1058	51.141 ± 0.4804	50.918 ± 0.2515
	10^5	N_2	1.8195 ± 0.0189	1.8357 ± 0.0036	1.7901 ± 0.0453	1.7939 ± 0.0095

Version	Fugacity, f / Pa		Absolute loading / molecules $\cdot$ cell^{-1}			
			conventional MC	CBMC	CFCMC	CB/CFCMC
RASPA2	10^6	CO_2	-	113.785 ± 0.109	112.341 ± 0.924	112.490 ± 0.270
	10^6	N_2	-	3.218 ± 0.012	3.189 ± 0.099	3.184 ± 0.038
RASPA3	10^6	CO_2	113.896 ± 0.456	113.891 ± 0.097	112.565 ± 0.750	112.387 ± 0.179
	10^6	N_2	3.179 ± 0.075	3.212 ± 0.010	3.137 ± 0.097	3.186 ± 0.023
RASPA2	10^7	CO_2	-	144.162 ± 0.245	142.456 ± 0.452	143.265 ± 0.436
	10^7	N_2	-	3.641 ± 0.018	3.794 ± 0.152	3.600 ± 0.097
RASPA3	10^7	CO_2	144.140 ± 0.311	144.065 ± 0.193	143.455 ± 0.838	142.664 ± 0.282
	10^7	N_2	3.647 ± 0.137	3.658 ± 0.071	3.439 ± 0.224	3.619 ± 0.095
RASPA2	10^8	CO_2	-	161.844 ± 0.274	162.201 ± 1.120	161.545 ± 0.338
	10^8	N_2	-	4.085 ± 0.143	3.863 ± 0.458	4.163 ± 0.181
RASPA3	10^8	CO_2	162.023 ± 0.546	161.697 ± 0.182	160.779 ± 0.888	160.426 ± 0.544
	10^8	N_2	3.967 ± 0.300	4.148 ± 0.079	4.024 ± 0.544	4.071 ± 0.178
RASPA2	10^9	CO_2	-	172.561 ± 0.534	172.053 ± 1.483	172.460 ± 1.049
	10^9	N_2	-	4.805 ± 0.244	4.944 ± 0.905	5.033 ± 0.564
RASPA3	10^9	CO_2	172.640 ± 2.412	172.864 ± 0.529	170.786 ± 0.983	171.337 ± 0.766
	10^9	N_2	4.768 ± 1.063	4.669 ± 0.196	5.128 ± 0.990	4.794 ± 0.538
RASPA2	10^{10}	CO_2	-	181.261 ± 0.970	181.171 ± 1.890	181.498 ± 0.823
	10^{10}	N_2	-	6.476 ± 0.633	6.434 ± 0.437	6.016 ± 0.703
RASPA3	10^{10}	CO_2	181.006 ± 0.922	181.654 ± 1.137	179.832 ± 1.368	179.928 ± 0.987
	10^{10}	N_2	6.754 ± 0.938	6.146 ± 0.726	6.611 ± 1.281	6.306 ± 1.248

TABLE S17: Absolute loading of an equimolar mixture of CO_2 and N_2 in $2 \times 2 \times 2$ MFI at 300K.

Version	Fugacity, f / Pa		Enthalpy of adsorption, H_{ads} / kJ · mol^{-1}			
			conventional MC	CBMC	CFCMC	CB/CFCMC
RASPA2	10^1	CO_2	-	-26.95 ± 0.13	-28.11 ± 2.00	-26.70 ± 1.84
	10^1	N_2	-	-15.17 ± 0.50	-11.63 ± 5.24	-13.75 ± 4.71
RASPA3	10^1	CO_2	-26.96 ± 0.20	-26.93 ± 0.08	-27.01 ± 0.45	-27.03 ± 0.18
	10^1	N_2	-15.19 ± 0.30	-15.21 ± 0.40	-14.67 ± 2.02	-14.78 ± 1.35
RASPA2	10^2	CO_2	-	-26.95 ± 0.04	-27.08 ± 0.39	-26.87 ± 0.44
	10^2	N_2	-	-14.99 ± 0.04	-14.74 ± 2.27	-14.80 ± 1.29
RASPA3	10^2	CO_2	-26.95 ± 0.07	-26.96 ± 0.02	-27.10 ± 0.14	-26.95 ± 0.07
	10^2	N_2	-15.18 ± 0.08	-15.11 ± 0.12	-14.85 ± 0.85	-15.11 ± 0.82
RASPA2	10^3	CO_2	-	-26.95 ± 0.05	-27.06 ± 0.22	-27.06 ± 0.08
	10^3	N_2	-	-15.15 ± 0.08	-15.46 ± 0.98	-15.18 ± 1.10
RASPA3	10^3	CO_2	-26.94 ± 0.06	-26.98 ± 0.02	-26.94 ± 0.11	-26.91 ± 0.09
	10^3	N_2	-15.18 ± 0.06	-15.14 ± 0.04	-15.17 ± 0.13	-15.11 ± 0.34
RASPA2	10^4	CO_2	-	-27.04 ± 0.02	-27.07 ± 0.09	-27.07 ± 0.08
	10^4	N_2	-	-15.20 ± 0.08	-15.43 ± 0.37	-15.11 ± 0.20
RASPA3	10^4	CO_2	-26.94 ± 0.06	-27.02 ± 0.05	-27.04 ± 0.09	-27.02 ± 0.13
	10^4	N_2	-15.18 ± 0.06	-15.24 ± 0.04	-15.16 ± 0.19	-15.18 ± 0.09
RASPA2	10^5	CO_2	-	-27.81 ± 0.07	-27.70 ± 0.14	-27.83 ± 0.03
	10^5	N_2	-	-15.80 ± 0.03	-15.74 ± 0.20	-15.76 ± 0.09
RASPA3	10^5	CO_2	-27.78 ± 0.15	-27.81 ± 0.06	-27.77 ± 0.07	-27.77 ± 0.05
	10^5	N_2	-15.71 ± 0.17	-15.79 ± 0.07	-15.67 ± 0.32	-15.69 ± 0.08

Version	Fugacity, f / Pa		Enthalpy of adsorption, H_{ads} / kJ · mol^{-1}			
			conventional MC	CBMC	CFCMC	CB/CFCMC
RASPA2	10^6	CO_2	-	-30.15 ± 0.14	-29.69 ± 0.14	-29.81 ± 0.27
	10^6	N_2	-	-16.98 ± 0.15	-16.53 ± 0.44	-16.74 ± 0.29
RASPA3	10^6	CO_2	-30.28 ± 0.48	-29.89 ± 0.24	-29.66 ± 0.44	-29.89 ± 0.24
	10^6	N_2	-17.15 ± 0.23	-16.76 ± 0.07	-16.78 ± 0.37	-16.76 ± 0.07
RASPA2	10^7	CO_2	-	-30.93 ± 0.24	-29.66 ± 0.77	-29.45 ± 0.87
	10^7	N_2	-	-16.86 ± 0.51	-16.12 ± 0.50	-15.64 ± 0.56
RASPA3	10^7	CO_2	-30.67 ± 0.54	-30.20 ± 0.23	-29.88 ± 0.82	-30.20 ± 0.23
	10^7	N_2	-16.67 ± 0.89	-16.19 ± 0.17	-16.32 ± 0.58	-16.19 ± 0.17
RASPA2	10^8	CO_2	-	-29.17 ± 0.70	-27.64 ± 1.62	-27.80 ± 1.51
	10^8	N_2	-	-15.23 ± 0.76	-13.48 ± 1.59	-13.49 ± 0.75
RASPA3	10^8	CO_2	-29.25 ± 0.92	-28.54 ± 0.16	-28.03 ± 0.76	-28.54 ± 1.60
	10^8	N_2	-14.69 ± 1.17	-14.25 ± 0.87	-14.30 ± 0.19	-14.25 ± 0.87
RASPA2	10^9	CO_2	-	-22.28 ± 1.46	-23.48 ± 2.44	-22.77 ± 0.81
	10^9	N_2	-	-7.95 ± 2.64	-8.90 ± 3.38	-9.36 ± 1.73
RASPA3	10^9	CO_2	-23.40 ± 0.41	-22.15 ± 2.47	-22.46 ± 4.03	-22.15 ± 2.47
	10^9	N_2	-9.62 ± 2.24	-8.65 ± 1.56	-8.74 ± 1.66	-8.65 ± 1.56
RASPA2	10^{10}	CO_2	-	-17.22 ± 1.52	-17.93 ± 3.33	-16.29 ± 1.55
	10^{10}	N_2	-	-3.88 ± 1.39	-5.27 ± 3.83	-3.85 ± 1.61
RASPA3	10^{10}	CO_2	-17.32 ± 1.701	-16.30 ± 1.52	-16.88 ± 4.01	-16.30 ± 1.52
	10^{10}	N_2	-5.98 ± 2.79	-2.86 ± 0.75	-5.01 ± 1.34	-2.86 ± 0.75

TABLE S18: Enthalpies of adsorption of an equimolar mixture of CO_2 and N_2 in $2 \times 2 \times 2$ MFI at 300K.

f / Pa	Measured fugacity CO_2, f/ Pa			Measured fugacity N_2, f/ Pa		
	Widom	CB/CFCMC		Widom	CB/CFCMC	
	$\left\langle e^{-\beta U^+} \right\rangle$	$\left\langle \ln \frac{P(\lambda=1)}{P(\lambda=0)} \right\rangle$	$\int \langle dU/d\lambda \rangle d\lambda$	$\left\langle e^{-\beta U^+} \right\rangle$	$\left\langle \ln \frac{P(\lambda=1)}{P(\lambda=0)} \right\rangle$	$\int \langle dU/d\lambda \rangle d\lambda$
10^1	$4.96 \cdot 10^0 \pm 0.20 \cdot 10^0$	$5.02 \cdot 10^0 \pm 0.15 \cdot 10^0$	$5.14 \cdot 10^0 \pm 0.14 \cdot 10^0$	$5.34 \cdot 10^0 \pm 0.71 \cdot 10^0$	$4.97 \cdot 10^0 \pm 0.75 \cdot 10^0$	$5.01 \cdot 10^0 \pm 0.75 \cdot 10^0$
10^2	$5.00 \cdot 10^1 \pm 0.07 \cdot 10^1$	$4.99 \cdot 10^1 \pm 0.26 \cdot 10^1$	$4.93 \cdot 10^1 \pm 0.22 \cdot 10^1$	$4.93 \cdot 10^1 \pm 0.03 \cdot 10^1$	$5.16 \cdot 10^1 \pm 0.23 \cdot 10^1$	$4.97 \cdot 10^1 \pm 0.40 \cdot 10^1$
10^3	$4.97 \cdot 10^2 \pm 0.04 \cdot 10^2$	$4.90 \cdot 10^2 \pm 0.13 \cdot 10^2$	$5.12 \cdot 10^2 \pm 0.16 \cdot 10^2$	$4.99 \cdot 10^2 \pm 0.09 \cdot 10^2$	$4.83 \cdot 10^2 \pm 0.17 \cdot 10^2$	$4.81 \cdot 10^2 \pm 0.16 \cdot 10^2$
10^4	$5.01 \cdot 10^3 \pm 0.04 \cdot 10^3$	$4.99 \cdot 10^3 \pm 0.03 \cdot 10^3$	$5.03 \cdot 10^3 \pm 0.02 \cdot 10^3$	$5.01 \cdot 10^3 \pm 0.05 \cdot 10^3$	$4.95 \cdot 10^3 \pm 0.02 \cdot 10^3$	$4.88 \cdot 10^3 \pm 0.05 \cdot 10^3$
10^5	$4.93 \cdot 10^4 \pm 0.03 \cdot 10^4$	$5.03 \cdot 10^4 \pm 0.19 \cdot 10^4$	$4.92 \cdot 10^4 \pm 0.16 \cdot 10^4$	$4.99 \cdot 10^4 \pm 0.03 \cdot 10^4$	$4.92 \cdot 10^4 \pm 0.14 \cdot 10^4$	$4.75 \cdot 10^4 \pm 0.12 \cdot 10^4$
10^6	$5.00 \cdot 10^5 \pm 0.04 \cdot 10^5$	$4.91 \cdot 10^5 \pm 0.18 \cdot 10^5$	$4.84 \cdot 10^5 \pm 0.25 \cdot 10^5$	$4.99 \cdot 10^5 \pm 0.03 \cdot 10^5$	$4.94 \cdot 10^5 \pm 0.09 \cdot 10^5$	$4.96 \cdot 10^5 \pm 0.23 \cdot 10^5$
10^7	$4.98 \cdot 10^6 \pm 0.16 \cdot 10^6$	$4.99 \cdot 10^6 \pm 0.07 \cdot 10^6$	$4.95 \cdot 10^6 \pm 0.32 \cdot 10^6$	$4.97 \cdot 10^6 \pm 0.02 \cdot 10^6$	$5.01 \cdot 10^6 \pm 0.14 \cdot 10^6$	$5.12 \cdot 10^6 \pm 0.18 \cdot 10^6$
10^8	$5.08 \cdot 10^7 \pm 0.34 \cdot 10^7$	$4.94 \cdot 10^7 \pm 0.15 \cdot 10^7$	$5.01 \cdot 10^7 \pm 0.07 \cdot 10^7$	$5.14 \cdot 10^7 \pm 0.11 \cdot 10^7$	$4.94 \cdot 10^7 \pm 0.08 \cdot 10^7$	$4.96 \cdot 10^7 \pm 0.20 \cdot 10^7$
10^9	$4.88 \cdot 10^8 \pm 0.64 \cdot 10^8$	$5.03 \cdot 10^8 \pm 0.18 \cdot 10^8$	$5.06 \cdot 10^8 \pm 0.35 \cdot 10^8$	$5.08 \cdot 10^8 \pm 0.37 \cdot 10^8$	$4.95 \cdot 10^8 \pm 0.17 \cdot 10^8$	$5.17 \cdot 10^8 \pm 0.16 \cdot 10^8$
10^{10}	$5.05 \cdot 10^9 \pm 0.18 \cdot 10^9$	$4.93 \cdot 10^9 \pm 0.14 \cdot 10^9$	$5.02 \cdot 10^9 \pm 0.24 \cdot 10^9$	$4.82 \cdot 10^9 \pm 0.72 \cdot 10^9$	$5.01 \cdot 10^9 \pm 0.11 \cdot 10^9$	$4.96 \cdot 10^9 \pm 0.37 \cdot 10^9$

TABLE S19: Imposed vs. measured fugacities of an equimolar mixture of CO_2 and N_2 in $2 \times 2 \times 2$ MFI at 300K using the CB/CFCMC method.

S-VIII. ADSORPTION SIMULATION OF CO_2 IN $1 \times 1 \times 1$ CU-BTC AT 300K

Simulation phase	Duration / cycles
Initialization cycles	250000
Equilibration cycles	250000
Production cycles	1000000

atom	ε/k_B / K	σ / Å	charge / e	mass / amu
Cu	2.5161	3.11369	1.248	63.546
O	48.1581	3.03315	-0.624	15.9994
C	47.8562	3.47299	0.494	12.0107
C	47.8562	3.47299	0.13	12.0107
C	47.8562	3.47299	-0.156	12.0107
H	7.64893	2.84642	0.156	1.0079
O_{co2}	85.671	3.017	-0.3256	15.9994
C_{co2}	29.933	2.745	0.6512	12.0

TABLE S20: Force field for CO2 in $2 \times 2 \times 2$ Cu-BTC at 300K. The MOF atoms are modeled using the UFF[6] force field for Cu, and DREIDING[9] for O, C, and H. The CO_2 model has bond-lengths of 1.149 Å, and has been taken from García-Sanchez et al.[7]. Cross terms are computed using the Lorentz-Berthelot mixing rules. The VDW interactions are neglected beyond the cutoff of 12 Å, and the potential is shifted to zero at the cutoff (i.e. no tail-corrections are applied). The Ewald precision is set to 10^{-6}. The positions for the Cu-BTC atoms have been taken from Chui et al.[10] and the structure has been kept rigid.

Version	Fugacity, f / Pa	Absolute loading / molecules cell^{-1}			
		Conventional MC	CBMC	CFCMC	CB/CFCMC
RASPA2	10^2	-	0.058 ± 0.001	0.053 ± 0.003	0.055 ± 0.002
RASPA3	10^2	0.057 ± 0.001	0.058 ± 0.001	0.056 ± 0.004	0.054 ± 0.002
RASPA2	10^3	-	0.565 ± 0.004	0.547 ± 0.014	0.547 ± 0.018
RASPA3	10^3	0.562 ± 0.005	0.566 ± 0.006	0.548 ± 0.016	0.543 ± 0.006
RASPA2	10^4	-	5.006 ± 0.045	4.849 ± 0.055	4.864 ± 0.043
RASPA3	10^4	5.010 ± 0.074	5.003 ± 0.010	4.857 ± 0.086	4.829 ± 0.023
RASPA2	10^5	-	31.568 ± 0.082	31.395 ± 0.426	31.372 ± 0.192
RASPA3	10^5	31.480 ± 0.164	31.512 ± 0.105	31.189 ± 0.282	31.401 ± 0.263
RASPA2	10^6	-	143.957 ± 0.249	142.745 ± 0.310	142.862 ± 0.289
RASPA3	10^6	143.442 ± 0.552	143.767 ± 0.227	143.708 ± 1.066	142.971 ± 0.332
RASPA2	10^7	-	181.509 ± 0.211	180.693 ± 0.719	180.480 ± 0.498
RASPA3	10^7	181.014 ± 0.749	181.556 ± 0.175	180.303 ± 1.173	180.535 ± 0.500
RASPA2	10^8	-	200.585 ± 0.268	199.608 ± 1.294	199.789 ± 0.455
RASPA3	10^8	200.715 ± 0.789	200.600 ± 0.177	200.375 ± 0.904	200.012 ± 0.256
RASPA2	10^9	-	215.106 ± 0.437	214.771 ± 0.938	215.748 ± 1.102
RASPA3	10^9	216.267 ± 1.716	215.037 ± 0.353	214.965 ± 1.824	214.805 ± 0.720

TABLE S21: Loading of CO_2 in $1 \times 1 \times 1$ Cu-BTC at 300K for different insertion methods and code versions.

f / Pa		μ_N	Bins											
	N		0	1	2									
10^2	RASPA2	0.06	945	53	2									
	RASPA3	0.04	957	42	1									
	N		0	1	2	3	4	5						
10^3	RASPA2	0.55	585	307	86	17	5	0						
	RASPA3	0.51	594	321	71	10	3	1						
	N		0-1	2-3	4-5	6-7	8-9	10-11	12-13	14-15				
10^4	RASPA2	4.87	31	234	378	249	90	17	1	0				
	RASPA3	4.71	33	251	391	242	63	18	1	1				
	N		16-18	19-21	22-24	25-27	28-30	31-33	34-36	37-39	40-42	43-45	46-48	49-51
10^5	RASPA2	31.39	3	18	64	139	222	230	162	97	44	14	5	2
	RASPA3	31.52	2	15	61	155	202	217	184	96	49	15	4	0
	N		119-122	123-126	127-130	131-134	135-138	139-142	143-146	147-150	151-154	155-158	159-162	
10^6	RASPA2	142.95	0	2	12	45	130	281	273	182	65	9	1	
	RASPA3	142.90	1	2	10	55	128	253	302	185	60	3	1	
	N		168-169	170-171	172-173	174-175	176-177	178-179	180-181	182-183	184-185	186-187	188-189	190-191
10^7	RASPA2	180.60	1	1	20	36	99	189	251	222	123	51	6	1
	RASPA3	180.52	0	1	16	37	115	205	249	212	112	36	15	2
	N		190-191	192-193	194-195	196-197	198-199	200-201	202-203	204-205	206-207	208-209		
10^8	RASPA2	199.45	3	10	51	155	277	296	157	40	10	1		
	RASPA3	199.98	0	3	47	134	229	301	198	81	6	1		
	N		208-209	210-211	212-213	214-215	216-217	218-219	220-221	222-223				
10^9	RASPA2	215.18	9	62	192	280	285	133	33	6				
	RASPA3	214.74	15	70	207	353	224	104	24	3				

TABLE S22: Particle number distribution for CO_2 in $1 \times 1 \times 1$ Cu-BTC at 300K for the CB/CFCMC insertion method.

Version	Fugacity, f / Pa	Simulation time / hh:mm			
		Conventional MC	CBMC	CFCMC	CB/CFCMC
RASPA2	10^2	-	3:03	5:60	6:18
RASPA3	10^2	0:47	1:08	2:23	2:32
RASPA2	10^3	-	4:40	6:05	7:26
RASPA3	10^3	1:20	1:48	2:25	2:36
RASPA2	10^4	-	7:03	6:11	6:56
RASPA3	10^4	2:10	2:48	2:29	2:44
RASPA2	10^5	-	12:50	11:54	13:11
RASPA3	10^5	3:48	4:41	4:13	4:39
RASPA2	10^6	-	80:22	72:40	77:10
RASPA3	10^6	18:51	23:06	20:45	22:27
RASPA2	10^7	-	100:49	89:46	94:50
RASPA3	10^7	21:08	25:58	23:13	25:25
RASPA2	10^8	-	104:38	94:49	99:09
RASPA3	10^8	21:21	26:12	23:41	25:58
RASPA2	10^9	-	107:28	97:01	102:55
RASPA3	10^9	21:12	26:18	23:42	26:14
RASPA2	Total	-	420:53	384:27	407:56
RASPA3	Total	90:36	111:59	102:49	112:35

TABLE S23: Simulation time of the GCMC simulation of CO_2 in $1 \times 1 \times 1$ Cu-BTC at 300K for different insertion methods and code versions.

Version	Fugacity, f / Pa	Enthalpy of adsorption, H_{ads} / kJ mol^{-1}			
RASPA2	10^2	-	-25.417 ± 0.092	-25.116 ± 0.802	-25.223 ± 0.540
RASPA3	10^2	-25.461 ± 0.123	-25.436 ± 0.074	-25.137 ± 0.289	-25.232 ± 0.181
RASPA2	10^3	-	-25.445 ± 0.044	-25.094 ± 0.156	-25.209 ± 0.088
RASPA3	10^3	-25.434 ± 0.017	-25.447 ± 0.053	-25.228 ± 0.226	-25.183 ± 0.089
RASPA2	10^4	-	-25.160 ± 0.043	-24.857 ± 0.122	-24.973 ± 0.163
RASPA3	10^4	-25.185 ± 0.093	-25.164 ± 0.090	-24.919 ± 0.246	-24.845 ± 0.151
RASPA2	10^5	-	-22.498 ± 0.141	-22.488 ± 0.268	-22.466 ± 0.072
RASPA3	10^5	-22.612 ± 0.062	-22.502 ± 0.077	-22.464 ± 0.082	-22.491 ± 0.161
RASPA2	10^6	-	-30.140 ± 0.238	-30.382 ± 0.122	-30.158 ± 0.195
RASPA3	10^6	-29.936 ± 0.361	-30.036 ± 0.080	-30.048 ± 0.461	-29.914 ± 0.353
RASPA2	10^7	-	-33.740 ± 0.356	-32.450 ± 1.107	-32.691 ± 0.770
RASPA3	10^7	-33.271 ± 0.590	-33.890 ± 0.405	-32.508 ± 0.849	-33.062 ± 0.994
RASPA2	10^8	-	-32.813 ± 1.665	-30.451 ± 1.748	-30.242 ± 1.127
RASPA3	10^8	-32.825 ± 1.439	-32.593 ± 0.828	-31.082 ± 2.033	-31.699 ± 2.419
RASPA2	10^9	-	-28.692 ± 3.390	-29.380 ± 3.139	-28.892 ± 2.621
RASPA3	10^9	-30.084 ± 2.330	-29.940 ± 0.845	-29.434 ± 3.818	-28.683 ± 3.247

TABLE S24: Enthalpy of adsorption of CO_2 in $1 \times 1 \times 1$ Cu-BTC at 300K for different insertion methods and code versions.

Fugacity, f / Pa	Chemical potential, μ / kJ mol^{-1}				
	Widom	CFCMC		CB/CFCMC	
	$\left\langle e^{-\beta U^+} \right\rangle$	$\left\langle \ln \frac{P(\lambda=1)}{P(\lambda=0)} \right\rangle$	$\int \langle \mathrm{d}U/\mathrm{d}\lambda \rangle \mathrm{d}\lambda$	$\left\langle \ln \frac{P(\lambda=1)}{P(\lambda=0)} \right\rangle$	$\int \langle \mathrm{d}U/\mathrm{d}\lambda \rangle \mathrm{d}\lambda$
10^2	-43.739 ± 0.054	-43.843 ± 0.186	-43.841 ± 0.176	-43.932 ± 0.096	-43.876 ± 0.126
10^3	-37.993 ± 0.061	-38.055 ± 0.087	-38.113 ± 0.050	-38.079 ± 0.134	-38.144 ± 0.054
10^4	-32.249 ± 0.042	-32.302 ± 0.043	-32.345 ± 0.055	-32.359 ± 0.079	-32.385 ± 0.029
10^5	-26.592 ± 0.077	-26.573 ± 0.070	-26.600 ± 0.068	-26.576 ± 0.074	-26.564 ± 0.050
10^6	-20.766 ± 0.016	-20.838 ± 0.087	-20.819 ± 0.069	-20.807 ± 0.091	-20.802 ± 0.069
10^7	-14.969 ± 0.108	-15.060 ± 0.096	-15.072 ± 0.125	-15.007 ± 0.035	-15.040 ± 0.112
10^8	-9.205 ± 0.299	-9.237 ± 0.077	-9.235 ± 0.189	-9.244 ± 0.069	-9.269 ± 0.146
10^9	-4.106 ± 0.812	-3.546 ± 0.057	-3.327 ± 0.141	-3.545 ± 0.049	-3.363 ± 0.166

TABLE S25: Excess chemical potential of CO_2 in $1 \times 1 \times 1$ Cu-BTC at 300K for different insertion methods computed with RASPA3.

Fugacity, f / Pa	Measured fugacity, f/ Pa				
	Widom	CFCMC		CB/CFCMC	
	$\left\langle e^{-\beta U^+} \right\rangle$	$\left\langle \ln \frac{P(\lambda=1)}{P(\lambda=0)} \right\rangle$	$\int \langle \mathrm{d}U/\mathrm{d}\lambda \rangle \mathrm{d}\lambda$	$\left\langle \ln \frac{P(\lambda=1)}{P(\lambda=0)} \right\rangle$	$\int \langle \mathrm{d}U/\mathrm{d}\lambda \rangle \mathrm{d}\lambda$
10^2	$1.0 \cdot 10^2 \pm 2.18 \cdot 10^0$	$9.63 \cdot 10^1 \pm 6.91 \cdot 10^0$	$9.64 \cdot 10^1 \pm 6.75 \cdot 10^0$	$9.29 \cdot 10^1 \pm 3.62 \cdot 10^0$	$9.5 \cdot 10^1 \pm 4.82 \cdot 10^0$
10^3	$1.01 \cdot 10^3 \pm 2.47 \cdot 10^1$	$9.8 \cdot 10^2 \pm 3.47 \cdot 10^1$	$9.58 \cdot 10^2 \pm 1.93 \cdot 10^1$	$9.71 \cdot 10^2 \pm 5.16 \cdot 10^1$	$9.46 \cdot 10^2 \pm 2.06 \cdot 10^1$
10^4	$1.01 \cdot 10^4 \pm 1.69 \cdot 10^2$	$9.84 \cdot 10^3 \pm 1.67 \cdot 10^2$	$9.67 \cdot 10^3 \pm 2.11 \cdot 10^2$	$9.62 \cdot 10^3 \pm 3.04 \cdot 10^2$	$9.52 \cdot 10^3 \pm 1.12 \cdot 10^2$
10^5	$9.71 \cdot 10^4 \pm 2.97 \cdot 10^3$	$9.78 \cdot 10^4 \pm 2.74 \cdot 10^3$	$9.68 \cdot 10^4 \pm 2.67 \cdot 10^3$	$9.77 \cdot 10^4 \pm 2.88 \cdot 10^3$	$9.82 \cdot 10^4 \pm 1.96 \cdot 10^3$
10^6	$1.0 \cdot 10^6 \pm 6.28 \cdot 10^3$	$9.75 \cdot 10^5 \pm 3.42 \cdot 10^4$	$9.83 \cdot 10^5 \pm 2.71 \cdot 10^4$	$9.87 \cdot 10^5 \pm 3.59 \cdot 10^4$	$9.89 \cdot 10^5 \pm 2.72 \cdot 10^4$
10^7	$1.03 \cdot 10^7 \pm 4.43 \cdot 10^5$	$9.89 \cdot 10^6 \pm 3.81 \cdot 10^5$	$9.84 \cdot 10^6 \pm 4.9 \cdot 10^5$	$1.01 \cdot 10^7 \pm 1.42 \cdot 10^5$	$9.97 \cdot 10^6 \pm 4.46 \cdot 10^5$
10^8	$1.03 \cdot 10^8 \pm 1.26 \cdot 10^7$	$1.02 \cdot 10^8 \pm 3.2 \cdot 10^6$	$1.02 \cdot 10^8 \pm 7.58 \cdot 10^6$	$1.02 \cdot 10^8 \pm 2.83 \cdot 10^6$	$1.01 \cdot 10^8 \pm 5.78 \cdot 10^6$
10^9	$7.99 \cdot 10^8 \pm 2.98 \cdot 10^8$	$1.0 \cdot 10^9 \pm 2.26 \cdot 10^7$	$1.09 \cdot 10^9 \pm 6.07 \cdot 10^7$	$1.0 \cdot 10^9 \pm 1.99 \cdot 10^7$	$1.08 \cdot 10^9 \pm 7.12 \cdot 10^7$

TABLE S26: Fugacity of CO_2 in $1 \times 1 \times 1$ Cu-BTC at 300K for different insertion methods computed with RASPA3.

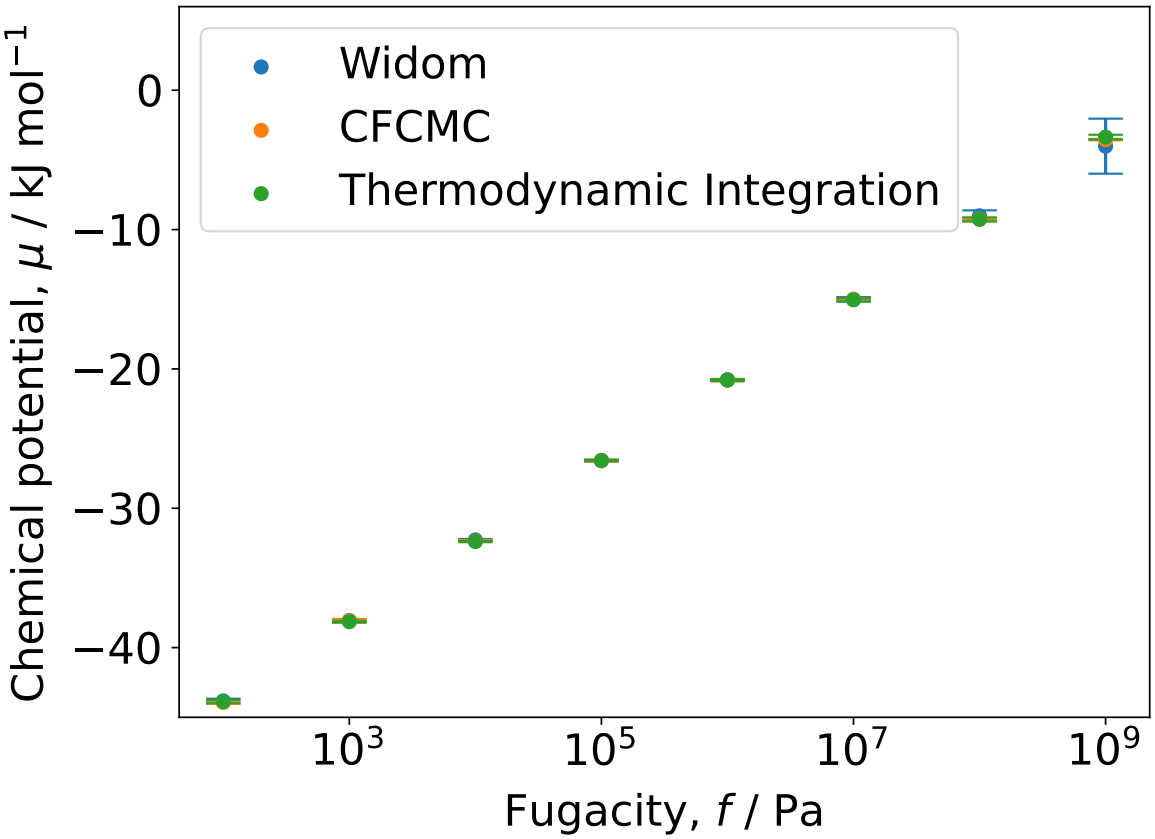

FIG. S7: Chemical potential of CO_2 at 300K insertion in Cu-BTC measured as a function of fugacity, computed with the Widom weight (blue), the Lambda weight (orange) and with thermodynamic integration (green).

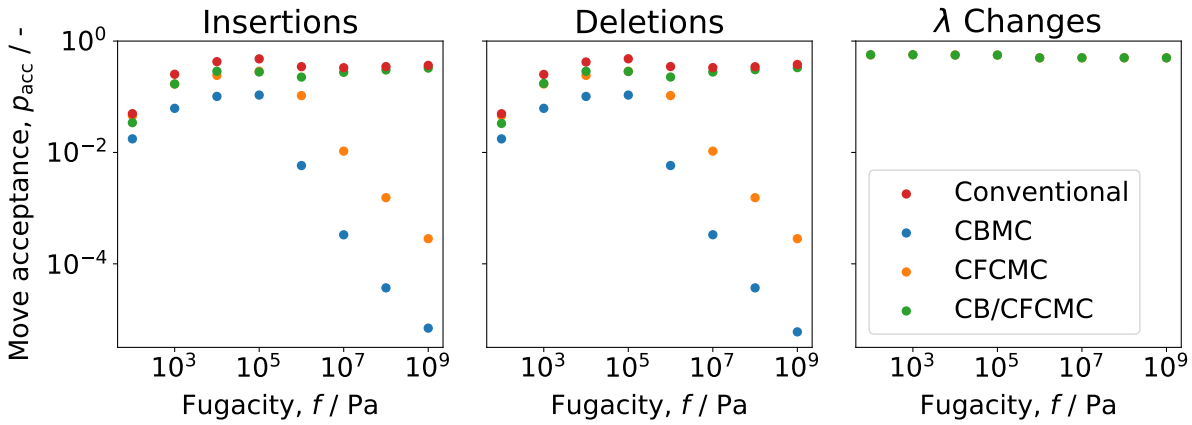

FIG. S8: Acceptance rate per attempted Monte-Carlo move for grand-canonical simulations of CO_2 at 300K in Cu-BTC performed with conventional swap (red), CBMC (blue), CFCMC (orange) and CB/CFCMC (green).

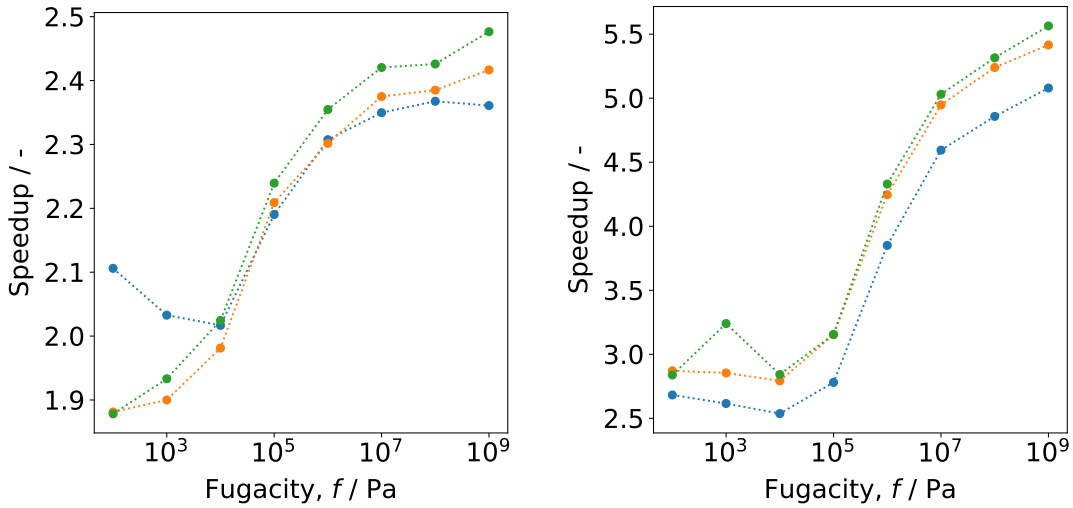

(a) Translation

(b) Widom

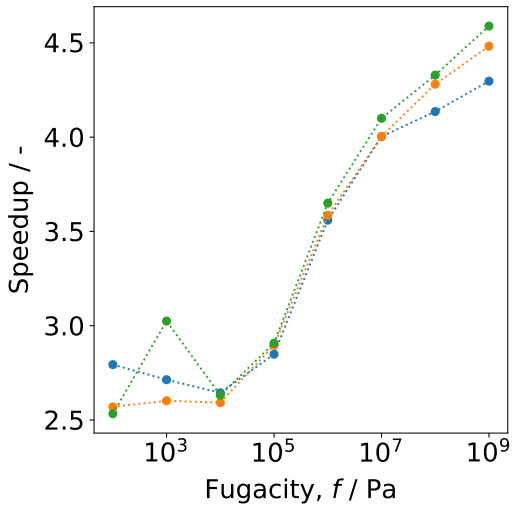

(c) Reinsertion (CBMC)

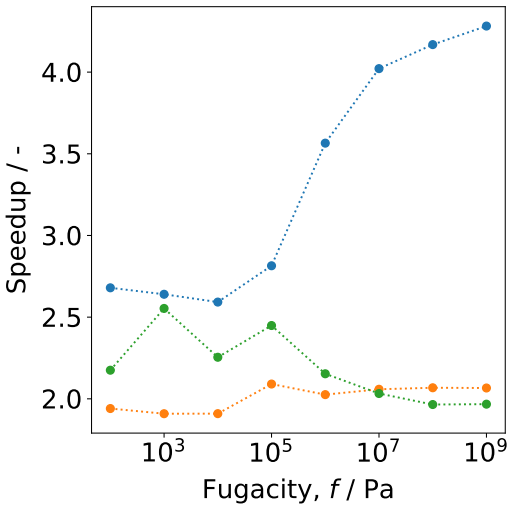

(d) Insertion

FIG. S9: Relative speedup of RASPA3 over RASPA2 evaluated per attempted Monte-Carlo move for grand-canonical simulations of CO_2 at 300K in Cu-BTC performed with CBMC (blue), CFCMC (orange) and CB/CFCMC (green).

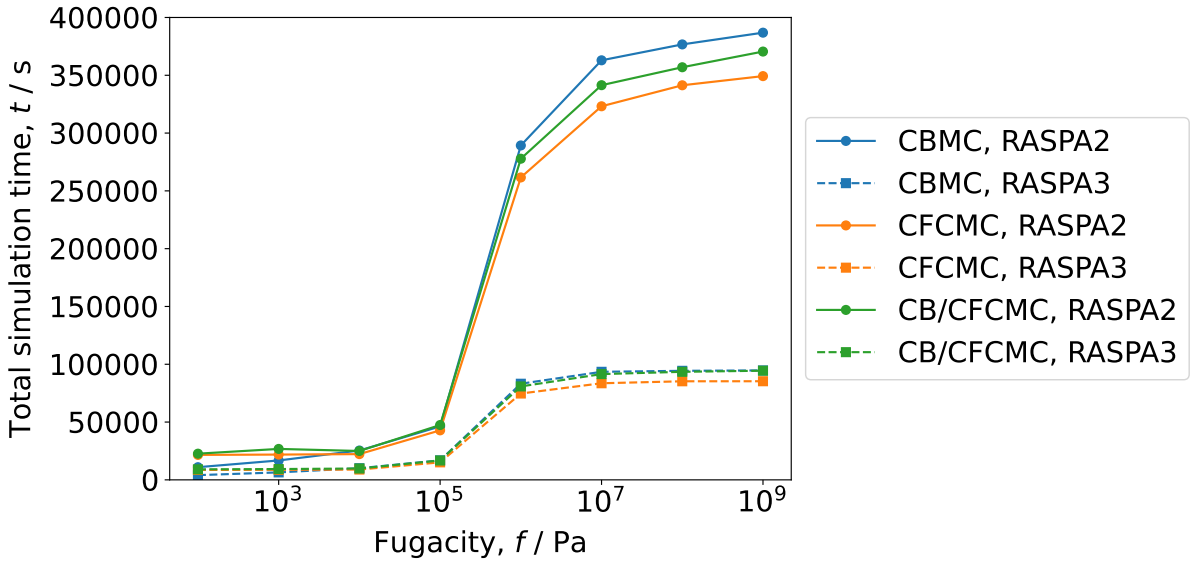

FIG. S10: Production simulation time per Grand-Canonical simulation of CO_2 at 300K in Cu-BTC performed with CBMC (blue), CFCMC (orange) and CB/CFCMC (green).

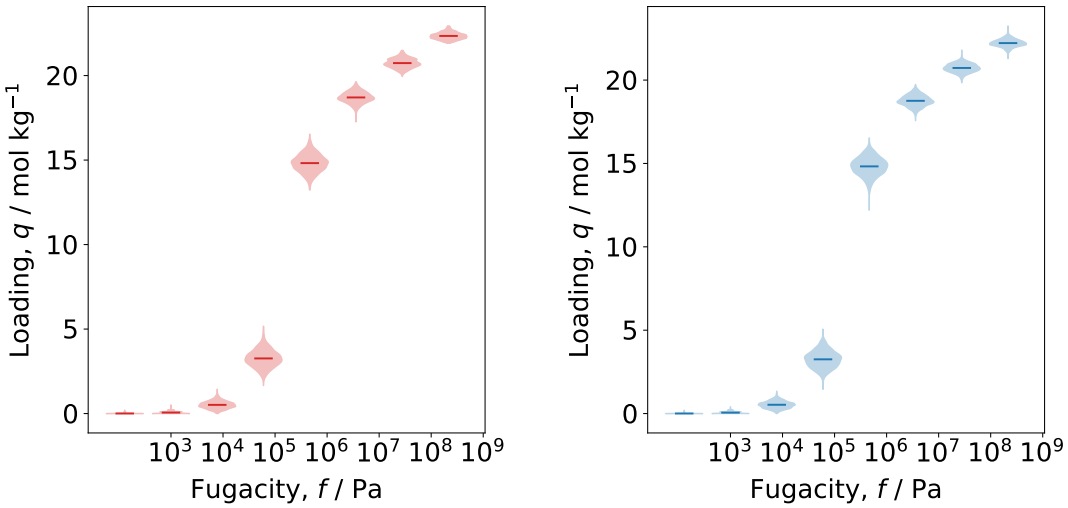

(a) Conventional

(b) CBMC

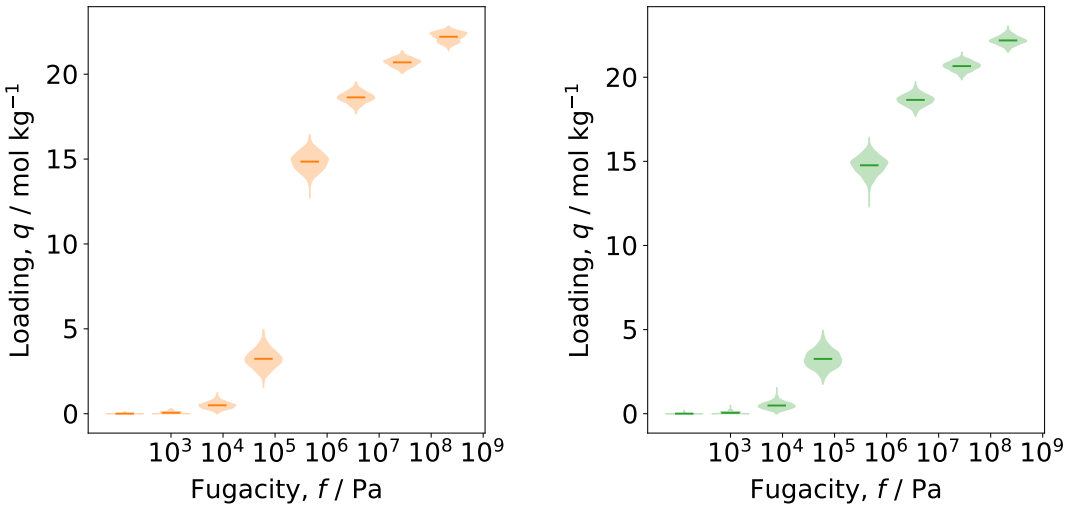

(c) CFCMC

(d) CB/CFCMC

FIG. S11: Particle distributions per Grand-Canonical adsorption simulation of CO_2 at 300K in Cu-BTC performed with CBMC (blue), CFCMC (orange) and CB/CFCMC (green).

S-IX. GIBBS-ENSEMBLE SIMULATION OF METHANE

Simulation phase	Duration / cycles
Initialization cycles	500000
Equilibration cycles	500000
Production cycles	1000000

atom	ε/k_B / K	σ / Å	charge / e	mass / amu
CH_4	158.5	3.72	-	16.04246

TABLE S27: Force field for VLE of CH_4. The CH_4 is modeled using the united-atom approach, and has been taken from Martin et al.[4]. The VDW interactions are neglected beyond the cutoff of 12 Å, and the potential is shifted to zero at the cutoff (i.e. no tail-corrections are applied). The Ewald charge computation has been omitted, since CH_4 is neutral.

Version	Temperature, T / K	Density / kg· m^{-3}			
		CBMC		CFCMC	
		vapor	liquid	vapor	liquid
RASPA2	100	0.750 ± 0.041	439.558 ± 0.174	0.747 ± 0.0306	438.888 ± 0.124
RASPA3	100	0.748 ± 0.018	439.480 ± 0.421	0.735 ± 0.074	439.330 ± 0.484
RASPA2	110	1.761 ± 0.036	424.771 ± 0.272	1.790 ± 0.053	424.496 ± 0.277
RASPA3	110	1.788 ± 0.024	425.130 ± 0.313	1.778 ± 0.148	424.260 ± 0.638
RASPA2	120	3.607 ± 0.059	409.484 ± 0.156	3.616 ± 0.146	408.707 ± 0.291
RASPA3	120	3.596 ± 0.049	409.451 ± 0.305	3.431 ± 0.141	408.944 ± 0.371
RASPA2	130	6.541 ± 0.080	393.110 ± 0.250	6.366 ± 0.106	392.735 ± 0.286
RASPA3	130	6.574 ± 0.158	393.145 ± 0.272	6.524 ± 0.156	392.802 ± 0.601
RASPA2	140	11.114 ± 0.091	376.022 ± 0.158	11.102 ± 0.277	375.564 ± 0.432
RASPA3	140	10.982 ± 0.105	375.668 ± 0.171	10.877 ± 0.339	375.384 ± 0.498
RASPA2	150	17.670 ± 0.127	356.808 ± 0.304	17.694 ± 0.291	356.889 ± 0.524
RASPA3	150	17.409 ± 0.207	356.540 ± 0.415	17.685 ± 0.167	356.479 ± 0.649
RASPA2	160	27.119 ± 0.288	335.179 ± 0.446	27.125 ± 0.608	335.505 ± 0.437
RASPA3	160	27.002 ± 0.163	335.312 ± 0.451	27.126 ± 0.580	334.809 ± 0.831

TABLE S28: Vapor/Liquid densities computed using Gibbs-ensemble VLE simulations of CH_4.

Version	Temperature, T / K	Pressure, p / bar			
		CBMC		CFCMC	
		vapor	liquid	vapor	liquid
RASPA2	100	0.382 ± 0.021	0.341 ± 0.114	0.392 ± 0.016	0.732 ± 0.693
RASPA3	100	0.382 ± 0.009	0.209 ± 1.241	0.375 ± 0.038	0.711 ± 1.031
RASPA2	110	0.972 ± 0.019	1.031 ± 0.144	1.009 ± 0.028	1.662 ± 0.481
RASPA3	110	0.987 ± 0.014	0.637 ± 0.297	0.980 ± 0.080	1.192 ± 0.879
RASPA2	120	2.119 ± 0.032	2.251 ± 0.363	2.157 ± 0.082	2.483 ± 0.760
RASPA3	120	2.111 ± 0.027	2.131 ± 1.022	2.017 ± 0.079	2.090 ± 0.576
RASPA2	130	4.024 ± 0.045	4.088 ± 0.320	3.968 ± 0.060	4.595 ± 0.360
RASPA3	130	4.043 ± 0.088	4.461 ± 0.837	4.013 ± 0.084	4.032 ± 0.524
RASPA2	140	7.024 ± 0.052	7.345 ± 0.366	7.072 ± 0.153	7.887 ± 0.484
RASPA3	140	6.957 ± 0.056	6.849 ± 1.213	6.887 ± 0.179	7.100 ± 0.786
RASPA2	150	11.271 ± 0.063	11.193 ± 0.270	11.345 ± 0.145	11.983 ± 0.414
RASPA3	150	11.137 ± 0.100	11.222 ± 0.618	11.263 ± 0.080	11.359 ± 0.399
RASPA2	160	17.073 ± 0.124	17.086 ± 0.454	17.136 ± 0.261	18.130 ± 0.355
RASPA3	160	17.013 ± 0.079	17.137 ± 0.645	17.054 ± 0.252	17.451 ± 0.842

TABLE S29: Vapor/Liquid pressures computed using Gibbs-ensemble VLE simulations of CH_4.

Version	Temperature, T / K	Chemical potential (Widom), μ / kJ· mol^{-1}			
		CBMC		CFCMC	
		vapor	liquid	vapor	liquid
RASPA2	100	-8.743 ± 0.036	-8.753 ± 0.050	-8.748 ± 0.018	-8.726 ± 0.216
RASPA3	100	-8.740 ± 0.019	-8.745 ± 0.055	-8.756 ± 0.083	-8.710 ± 0.119
RASPA2	110	-8.867 ± 0.013	-8.847 ± 0.046	-8.847 ± 0.0163	-8.880 ± 0.0694
RASPA3	110	-8.847 ± 0.012	-8.829 ± 0.049	-8.853 ± 0.071	-8.836 ± 0.030
RASPA2	120	-9.002 ± 0.012	-8.992 ± 0.0138	-9.001 ± 0.038	-8.997 ± 0.019
RASPA3	120	-9.000 ± 0.012	-8.993 ± 0.025	-9.043 ± 0.036	-8.981 ± 0.059
RASPA2	130	-9.180 ± 0.011	-9.173 ± 0.011	-9.204 ± 0.016	-9.183 ± 0.022
RASPA3	130	-9.168 ± 0.021	-9.172 ± 0.025	-9.176 ± 0.022	-9.166 ± 0.029
RASPA2	140	-9.366 ± 0.007	-9.355 ± 0.014	-9.368 ± 0.024	-9.364 ± 0.023
RASPA3	140	-9.369 ± 0.008	-9.368 ± 0.017	-9.378 ± 0.027	-9.371 ± 0.022
RASPA2	150	-9.584 ± 0.005	-9.580 ± 0.009	-9.583 ± 0.013	-9.577 ± 0.010
RASPA3	150	-9.588 ± 0.010	-9.588 ± 0.006	-9.576 ± 0.008	-9.578 ± 0.014
RASPA2	160	-9.821 ± 0.007	-9.811 ± 0.008	-9.822 ± 0.018	-9.804 ± 0.010
RASPA3	160	-9.814 ± 0.004	-9.815 ± 0.005	-9.812 ± 0.014	-9.814 ± 0.013

TABLE S30: Vapor/Liquid chemical potentials computed using Gibbs-ensemble VLE simulations of CH_4.

Version	Temperature, T / K	Acceptance ratios / -						λ-occupancy / -	
		vapor			liquid			vapor	liquid
		swap	shuffle	λ-move	swap	shuffle	λ-move		
RASPA2	100	0.4080	0.1257	0.5001	0.3801	0.1171	0.5032	0.4836	0.5165
RASPA3	100	0.6781	0.1447	0.5032	0.5850	0.1249	0.5026	0.4628	0.5372
RASPA2	110	0.4332	0.1307	0.5005	0.4151	0.1252	50.167	0.4901	0.5099
RASPA3	110	0.7049	0.1467	0.5001	0.6155	0.1282	0.5014	0.4657	0.5343
RASPA2	120	0.4607	0.1374	0.4999	0.4328	0.1290	0.4997	0.4845	0.5155
RASPA3	120	0.6813	0.1475	0.5008	0.6740	0.1460	0.5005	0.4976	0.5024
RASPA2	130	0.4857	0.1442	0.5013	0.4535	0.1346	0.5002	0.4831	0.5169
RASPA3	130	0.7255	0.1534	0.5001	0.6605	0.1397	0.5009	0.4770	0.5230
RASPA2	140	0.4755	0.1496	0.4998	0.4837	0.1522	0.5000	0.5052	0.4948
RASPA3	140	0.7171	0.1554	0.5002	0.6896	0.1494	0.5021	0.4901	0.5099
RASPA2	150	0.5034	0.1606	0.4998	0.4936	0.1575	0.5002	0.4964	0.5036
RASPA3	150	0.7221	0.1598	0.4999	0.6965	0.1543	0.4993	0.4911	0.5089
RASPA2	160	0.5154	0.1725	0.5000	0.5075	0.1700	0.4998	0.4985	0.5015
RASPA3	160	0.6860	0.1599	0.5009	0.7179	0.1674	0.5012	0.5109	0.4891

TABLE S31: Vapor/Liquid acceptance ratios of the CFCMC-Gibbs-ensemble VLE simulations of CH_4. The λ-occupancy is the fraction of the time that the fractional molecule spends in the vapor- and liquid-phase, respectively.

Temperature, T / K	Chemical potential, μ / kJ· mol^{-1}					
	Vapor			Liquid		
	$\left\langle e^{-\beta U^+} \right\rangle$	$\left\langle \ln \frac{P(\lambda=1)}{P(\lambda=0)} \right\rangle$	$\int \langle dU/d\lambda \rangle d\lambda$	$\left\langle e^{-\beta U^+} \right\rangle$	$\left\langle \ln \frac{P(\lambda=1)}{P(\lambda=0)} \right\rangle$	$\int \langle dU/d\lambda \rangle d\lambda$
100	-8.714 ± 0.073	-8.717 ± 0.079	-8.713 ± 0.073	-8.702 ± 0.087	-8.703 ± 0.104	-8.815 ± 0.101
110	-8.850 ± 0.037	-8.869 ± 0.039	-8.848 ± 0.038	-8.842 ± 0.022	-8.843 ± 0.058	-8.941 ± 0.037
120	-8.998 ± 0.040	-8.987 ± 0.057	-8.997 ± 0.042	-9.003 ± 0.046	-8.982 ± 0.047	-9.094 ± 0.030
130	-9.138 ± 0.010	-9.139 ± 0.046	-9.135 ± 0.009	-9.153 ± 0.024	-9.161 ± 0.030	-9.226 ± 0.038
140	-9.364 ± 0.019	-9.351 ± 0.047	-9.363 ± 0.016	-9.369 ± 0.017	-9.380 ± 0.019	-9.444 ± 0.039
150	-9.578 ± 0.017	-9.590 ± 0.044	-9.577 ± 0.017	-9.560 ± 0.011	-9.556 ± 0.029	-9.589 ± 0.056
160	-9.810 ± 0.007	-9.811 ± 0.014	-9.799 ± 0.019	-9.862 ± 0.059	-9.833 ± 0.049	-9.862 ± 0.059

TABLE S32: Measured chemical potentials for RASPA3 Gibbs-ensemble simulations of CH_4.

S-X. DIFFUSION IN $2 \times 2 \times 2$ IN IRMOF-1 AT 298K

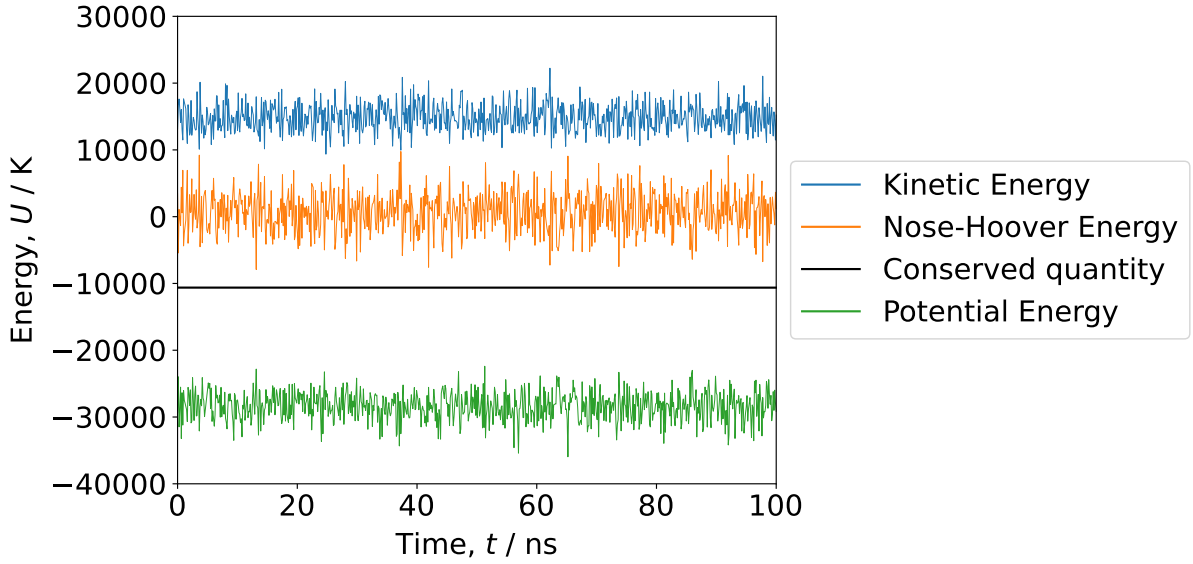

FIG. S12: Molecular dynamics energy conservation of 80 methane in $2 \times 2 \times 2$ IRMOF-1 at 298K: kinetic energy, Nose-Hoover energy, and potential energy should add up to a conserved quantity.

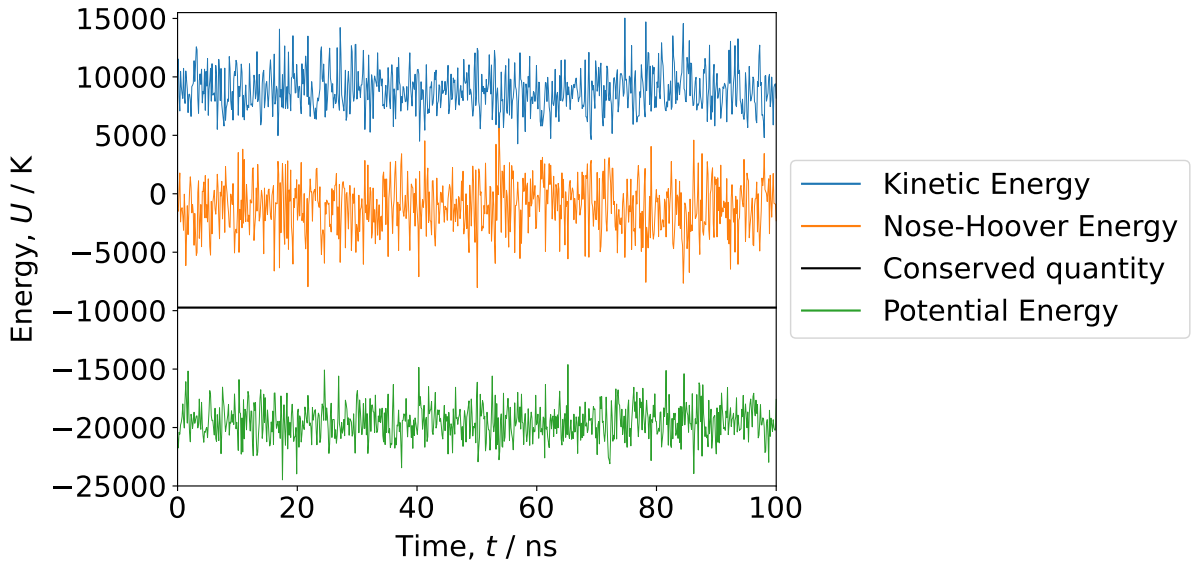

FIG. S13: Molecular dynamics energy conservation of 80 CO_2 in $2 \times 2 \times 2$ IRMOF-1 at 298K: kinetic energy, Nose-Hoover energy, and potential energy should add up to a conserved quantity.

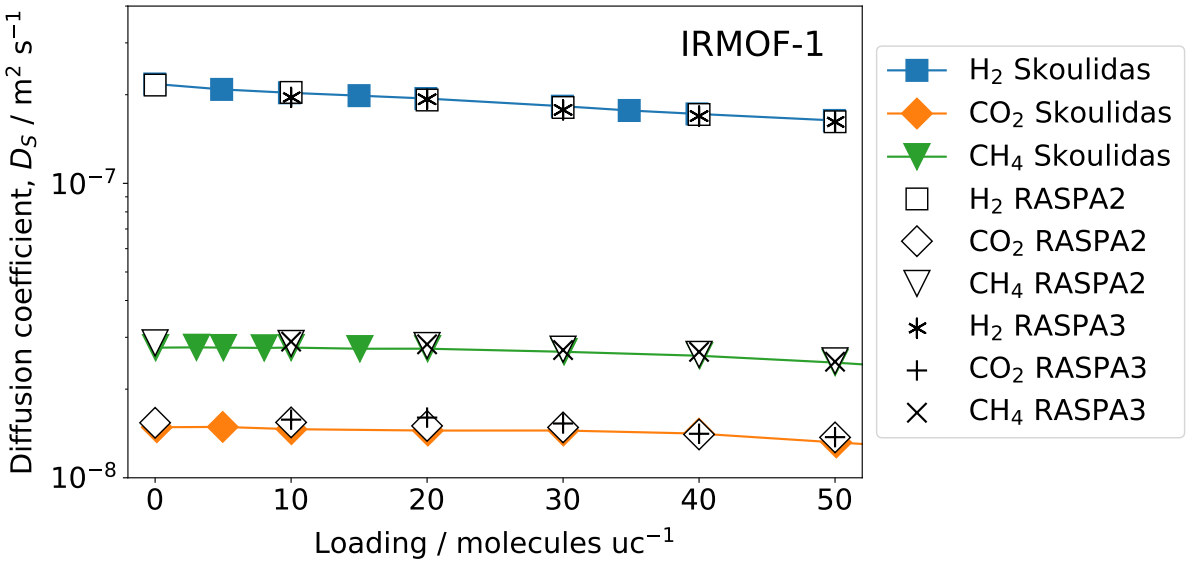

FIG. S14: Simulated diffusivities of small gasses in IRMOF-1 at 298K. Closed symbols, previous results of Skoulidas and Sholl[11]; open symbols, previous results for RASPA2[12]; cross/plus/star, this work using RASPA3.

REFERENCES

[1] https://www.nist.gov/mml/csd/chemical-informatics-group/spce-water-reference-calculations-non-cuboid-cell-10a-cutoff.

[2] D. Dubbeldam, E. Beerdsen, T. J. H. Vlugt, and B. Smit, "Molecular simulation of loading-dependent diffusion in nanoporous materials using extended dynamically corrected transition state theory," The Journal of Chemical Physics **122**, 224712 (2005), https://pubs.aip.org/aip/jcp/article-pdf/doi/10.1063/1.1924548/15370221/224712_1_online.pdf.

[3] P. Bai, M. Tsapatsis, and J. I. Siepmann, "TraPPE-zeo: Transferable potentials for phase equilibria force field for all-silica zeolites," J. Phys. Chem. C **117**, 24375–24387 (2013).

[4] M. G. Martin, A. P. Thompson, and T. M. Nenoff, "Effect of pressure, membrane thickness, and placement of control volumes on the flux of methane through thin silicalite membranes: A dual control volume grand canonical molecular dynamics study," J. Chem. Phys. **114**, 7174–7181 (2001).

[5] A. Martin-Calvo, E. Garcia-Perez, A. Garcia-Sanchez, R. Bueno-Perez, S. Hamada, and S. Calero, "Effect of air humidity on the removal of carbon tetrachloride from air using Cu–BTC metal-organic framework," Phys. Chem. Chem. Phys. **13**, 11165–11174 (2011).

[6] A. Rappé, C. Casewit, K. Colwell, W. Goddard, and W. Skiff, "UFF, a full periodic table force field for molecular mechanics and molecular dynamics simulations," J. Am. Chem. Soc. **114**, 10024–10035 (1992).

[7] A. García-Sanchez, C. O. Ania, J. B. Parra, D. Dubbeldam, T. J. H. Vlugt, R. Krishna, and S. Calero, "Transferable force field for carbon dioxide adsorption in zeolites," J. Phys. Chem. C **113**, 8814–8820 (2009).

[8] H. van Koningsveld, H. van Bekkum, and J. C. Jansen, "On the location and disorder of the tetrapropylammonium (TPA) ion in zeolite ZSM-5 with improved framework accuracy," Acta Cryst. **B43**, 127–132 (1987).

[9] S. Mayo, B. Olafson, and W. Goddard, "DREIDING: A generic force field for molecular simulations," J. Phys. Chem. **94**, 8897–8909 (1990).

[10] S. Chui, S. Lo, J. Charmant, A. Orpen, and I. Williams, "A chemically functionalizable nanoporous material [Cu-3(TMA)(2)(H2O)(3)](n)," Science **283**, 1148–1150 (1999).

[11] A. Skoulidas and D. Sholl, "Self-diffusion and transport diffusion of light gases in metal-organic framework materials assessed using molecular dynamics simulations," J. Phys. Chem. B. **109**,

15760 – 15768 (2005).

[12]D. Dubbeldam, S. Calero, D. E. Ellis, and R. Q. Snurr, "RASPA: Molecular simulation software for adsorption and diffusion in flexible nanoporous materials," **42**, 81–101 (2016).